



Research paper

Investigating age-related muscle force adaptations in males and females during sit-to-walk transition motion using EMG-informed modeling

Zakia Hussain^a, Alpha Agape Gopalai^{a,*}, Siti Anom Ahmad^b, Mazatulfazura Sf Binti Salim^c, Darwin Gouwanda^a, Pei-Lee Teh^d

^a Medical Engineering & Technology Research Hub, School of Engineering, Monash University Malaysia, Selangor, 47500, Malaysia

^b Department of Electrical and Electronic Engineering, Faculty of Engineering, Universiti Putra Malaysia, Serdang, Selangor, 43400, Malaysia

^c Department of Rehabilitation Medicine, Faculty of Medicine and Health Sciences, Universiti Putra Malaysia, Serdang, Selangor, 43400, Malaysia

^d Gerontechnology Laboratory, School of Business, Monash University Malaysia, Selangor, 47500, Malaysia



ARTICLE INFO

Keywords:

Aging
Mobility
Muscle forces
Neuromusculoskeletal modelling
Sex-differences
Sit-to-walk

ABSTRACT

Background: The sit-to-walk (STW) transition is essential for mobility but deteriorates with age due to declining muscle strength, balance, and postural control. This study hypothesizes that age- and sex-related variations in muscle forces during STW lead to altered muscle recruitment strategies, reflecting compensatory mechanisms. When these compensations are no longer adequate, mobility limitations may occur.

Methods: This study involved 65 healthy adults (32 males and 33 females) from three age groups. Motion capture and surface electromyography (sEMG) data were used to develop an EMG-informed neuromusculoskeletal model for estimating muscle forces. Age and sex-related variations in muscle forces were analyzed using Generalized Linear Mixed Modeling (GLMM).

Results: The findings reveal consistent recruitment of primary STW muscles across all age-sex subgroups. The *vasti*, *gluteus maximus*, *gluteus medius*, *dorsiflexors*, and *soleus* generated the highest average muscle forces during STW. However, older adults consistently generated lower forces in these muscles during rising (except for the *soleus*). Despite this, phase durations were like other groups, with increased ankle plantarflexor (except *gastrocnemius*) and hip abductors (*gluteus medius*) forces to support gait transition. These findings indicate compensation in healthy aging involves variations in muscle force production rather than altered muscle recruitment strategies. Moreover, females exhibited more pronounced age-related muscle force changes than males during gait initiation.

Conclusion: Significant age- and sex-specific variations in muscle forces across STW phases highlight the need for biomechanically informed interventions to preserve muscle health and reduce functional decline. Targeted interventions should focus on strengthening STW muscles and not just knee extensors to enhance mobility. For example, exercises like Tai Chi, known to improve dynamic stability during gait initiation, can benefit females across age groups.

1. Introduction

One of the significant challenges in healthy aging is maintaining functional mobility and quality of life. As we age, the ability to safely perform activities of daily living (ADL) deteriorates, making us susceptible to disability, disease, and reduced well-being [1,2]. One such essential ADL is the sit-to-walk (STW) transition motion, where the ability to rise from a seated position to a walking stance becomes significantly challenging due to declining muscle strength, balance, and

postural control [3–5].

The age-related decline in muscle strength affects the ability to rise up, with muscle strength being critical for successful chair-rise movements [6,7]. Consequently, skeletal muscle health is a key predictor of an individual's overall mobility and longevity [8,9]. Strengthening skeletal muscles like knee extensors (*vastus lateralis*, *medialis*, *intermedius*, and *rectus femoris*) is often recommended to improve STW performance in older adults [5,10]. However, focusing solely on these muscles does not necessarily improve rising from a seated position [11,

* Corresponding author.

E-mail address: alpha.agape@monash.edu (A.A. Gopalai).

<https://doi.org/10.1016/j.rineng.2025.104660>

Received 27 September 2024; Received in revised form 15 January 2025; Accepted 17 March 2025

Available online 17 March 2025

2590-1230/© 2025 The Authors. Published by Elsevier B.V. This is an open access article under the CC BY license (<http://creativecommons.org/licenses/by/4.0/>).

Table 1
Demographics of the participants.

	Mean (Standard deviation)					
	Young adults (19 - 30 years)		Middle-aged adults (31- 54 years)		Older adults (aged 55 and above)	
	M (n = 15)	F (n = 12)	M (n = 13)	F (n = 7)	M (n = 4)	F (n = 14)
Age (years)	23.06 (2.91)	22.25 (2.67)	38.54 (5.70)	41.71 (6.16)	64.75 (6.85)	63.79 (3.82)
Height (cm)	172.21 (3.44)	155.96 (4.88)	170.90 (7.23)	154.47 (6.70)	165 (1.36)	155.28 (5.34)
Body mass (kg)	71.65 (13.18)	49.38 (6.26)	77.44 (16.10)	56.71 (10.13)	66.59 (2.19)	58.58 (11.17)

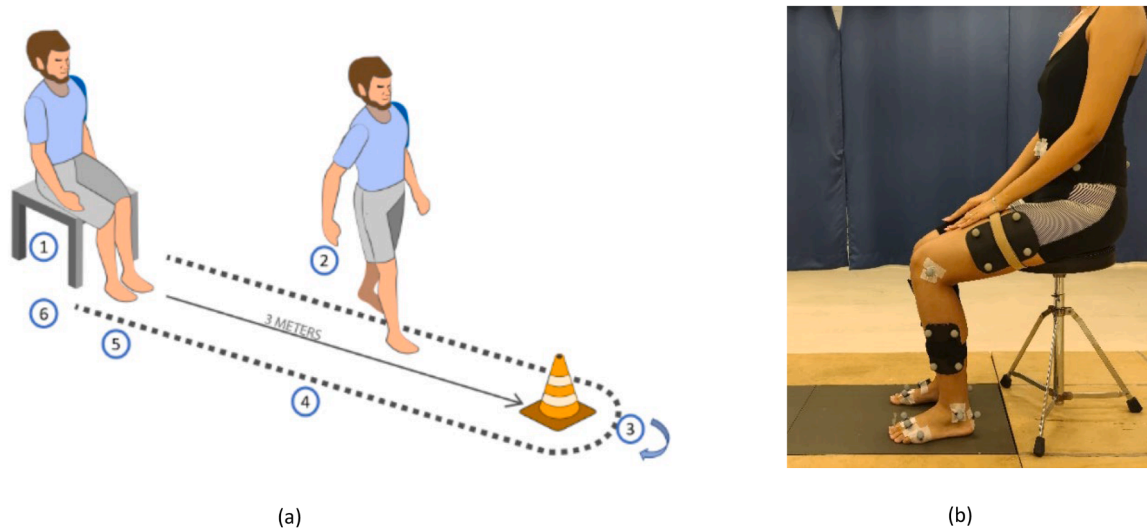


Fig. 1. (a) TUG test [75] (b) Initial seated position of a participant.

[12], as it overlooks other crucial muscles including the *gluteus maximus*, *adductor magnus*, *soleus*, *gastrocnemius*, and *tibialis anterior*. These muscles are vital in generating adequate moments for forward and vertical acceleration while rising up [13]. Specifically, the *gluteus maximus* predominantly drives hip extension, while the *vasti* are key contributors to knee extension during rising [14,15]. Understanding the specific contributions of distinct lower limb muscles during STW is essential for designing targeted strategies to improve STW performance.

Hence, this study aims to investigate muscle forces during different phases of STW and characterize their variations across young, middle-aged, and older males and females. While muscle force profiles are the primary outcome of this study, they are intrinsically linked to key muscle functions such as movement generation [16] and posture maintenance [17] during tasks like STW. Analyzing muscle forces is essential for understanding muscle function and developing advanced treatments for movement disorders [18,19]. While some studies have used EMG to examine lower limb muscle activity in healthy older adults [10,20], muscle excitation alone does not directly quantify muscle forces [18]. Additionally, lower limb muscle forces during similar transitional motions like sit-to-stand (STS), have been estimated using static optimization [21–23], which assumes uniform muscle activation strategies across individuals. However, variations in muscle forces across STW phases, especially age-related adaptations in muscle recruitment strategies, remain unexplored.

These recruitment strategies are influenced by muscle redundancy, where multiple muscles can perform similar functions, resulting in compensation [24]. In healthy aging, compensation through altered muscle recruitment may occur due to the uneven decline in strength across muscle groups [13]. This study hypothesizes that 1) muscle force profiles will vary across age and sex subgroups during different STW phases and 2) these variations will reflect altered muscle recruitment strategies in healthy aging. Given the anatomical complexity of the

lower limb, computational modeling is essential for estimating individual muscle forces and exploring how coordination changes with age during movement.

Recent studies indicate that males and females develop muscle pathologies differently [25–27], with females being more susceptible to reduced independence due to muscle mass loss with aging [28]. Yet studies have predominantly focused on male muscle function, leaving a significant gap in understanding female muscle function in computational modelling [29,30]. Further evidence highlights sex-based differences in muscle mass and strength [31–35]. By addressing this gap, this study uniquely explores how age and sex influence muscle forces during STW, offering insights into compensatory strategies in healthy aging.

To estimate these muscle forces, an electromyography (EMG)-informed neuromusculoskeletal (NMS) model is used, accounting for subject-specific muscle excitation patterns. This method offers a more precise representation of muscle physiology [36], resulting in more accurate muscle force estimates compared to commonly used optimization-based studies [37]. By analyzing healthy adults' subject-specific muscle force profiles, this work seeks to establish a benchmark for detecting and assessing NMS impairments. These findings could inform personalized interventions to maintain functional mobility and independence in muscle-impaired individuals.

2. Materials and methods

2.1. Participants

Sixty-five healthy adults, 32 males (M) and 33 females (F) across three age groups, volunteered to participate in this study. All participants had no prevalent musculoskeletal impairment that could hinder their ability to perform the experimental tasks. The Monash University Human Research Ethics Committee approved the study methodology,

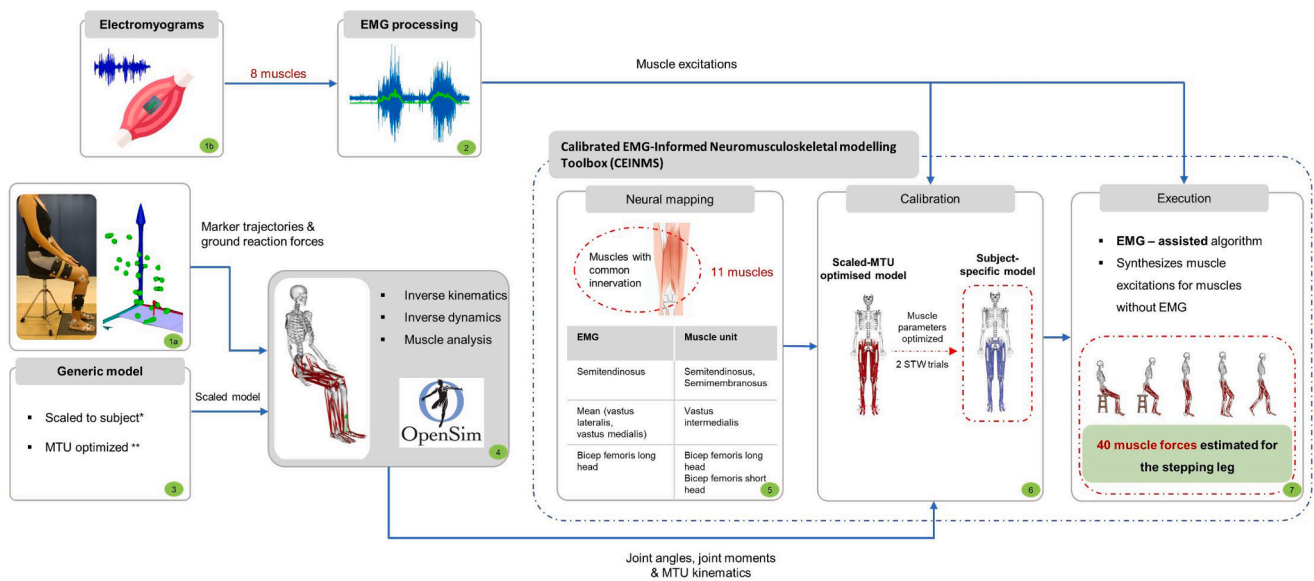


Fig. 2. Overview of EMG-informed model. The first step is the STW 1a) marker trajectories, ground reaction forces and 1b) electromyogram (EMG) data collection followed by 2) EMG processing, 3) a generic model (Rajagopal[45]) was linearly scaled and musculotendon units (MTUs) were morphometrically scaled as per [49], 4) processed motion capture and force plate data was used to calculate the joint angles, joint moments, and MTU kinematics, in OpenSim. The last step involves using CEINMS toolbox beginning with 5) neural mapping— 8 experimental EMGs are mapped to 11 MTUs with same innervation, 6) calibration to adjust MTU parameters and 7) execution step to estimate 40 MTU forces of the stepping leg for each subject.

and all participants provided their informed written consent before the start of the experiment. The descriptive distribution of subject demography is shown in Table 1.

2.2. Instrumentation

Lower body motion capture data was collected using six Oqus Qualisys optical cameras (Qualisys, Inc., Goteborg, Sweden) sampled at 200 Hz. Ground reaction forces (GRF) were measured using three synchronized force platforms (Bertec Inc., Columbus, USA) embedded in a wooden platform sampled at 1000 Hz. Surface EMG (sEMG) data was obtained using wireless Trigno Avanti and Trigno Duo sensors, sampled at its default setting of 1259 Hz and 1778 Hz, respectively (Trigno, Delsys Inc., Boston, USA). To ensure synchronized start and stop times across all systems—optical cameras, force plates, and the Delsys Trigno system—a Delsys Trigger Module was employed.

2.3. Procedures

Thirty-six retroreflective markers (12.5 mm) were placed on the participants' pelvis and lower limb anatomical landmarks following the Calibrated Anatomical System Technique (CAST) [38]. Skin was prepared for EMG sensor placement by cleaning with alcohol swabs to enhance electrode-skin contact. Electrodes were placed on eight muscles of the dominant leg (defined as kicking leg) using surgical tape, following Surface Electromyography for the Non-Invasive Assessment of Muscle (SENIAM) guidelines [39]. The included muscles were *tibialis anterior*, *gastrocnemius medialis*, *gastrocnemius lateralis*, *rectus femoris*, *vastus lateralis*, *vastus medialis*, *semitendinosus*, and *bicep femoris long head*, chosen based on their ease and practical electrode placement. Maximum voluntary contractions (MVCs) were also performed so that subjects' EMG data could be normalized.

STW trials were conducted as part of the Timed Up and Go (TUG) test [5] (Fig. 1a). Participants sat barefoot on a height-adjustable, armless, and backless stool positioned in front of the first force plate (Fig. 1b). Their hands rested on their thighs to avoid obstructing markers, while their feet were placed on the first force plate, and their knees were bent at approximately 90° angle. Participants rose, walked 3 m, turned

around, walked back, and sat down. Each participant performed five successful TUG trials, with STW then extracted from the forward movement. Participants' STW movement was not restricted, allowing for both natural movements and any compensatory action. Trials were omitted if participants failed to land on a single force plate or if a foot crossed over more than one force plate.

2.4. Data processing

EMG data was down sampled to 1000 Hz to match the force plate frequency and reduce the number of data points for uniformity. This also ensured compliance with the Nyquist theorem, which requires a sampling rate at least twice the highest frequency components (400–500 Hz) to prevent aliasing [40,41]. Experimental data were processed using the MOtoNMS MATLAB toolbox [42]. Marker trajectories and GRF data were filtered using a fourth-order low-pass Butterworth zero-lag filter with a cut-off frequency of 5 Hz and 20 Hz, respectively. EMG signals were high-pass-filtered at 30 Hz, full-wave rectified, and low-pass-filtered at 6 Hz [43]. The resulting EMG linear envelopes were normalized against each muscle's maximum instantaneous value (based on MVC readings), across all five STW trials. All experimental data, including marker trajectories, force data, and EMG have been made available publicly [44].

2.5. Musculoskeletal (MSK) modeling

A generic full-body MSK model with 80 muscle-tendon units (MTUs) [45]—40 per leg—was used in OpenSim 3.3 [46] to simulate lower-body STW movements. These MTUs are modeled as a single entity using the Hill-type muscle model, where muscles and tendons act in series [47]. In this model, the forces generated by muscle fibers are transmitted through tendons to the skeleton, producing movement. Thus, "muscle forces" in this study refers to the forces estimated within the musculotendon units.

The MSK model was scaled to match each participant's anthropometry using static trial data. Muscle force prediction is sensitive to subject-specific optimal fiber and tendon slack lengths, which were scaled using an optimization technique for all participants [48,49]. Processed motion

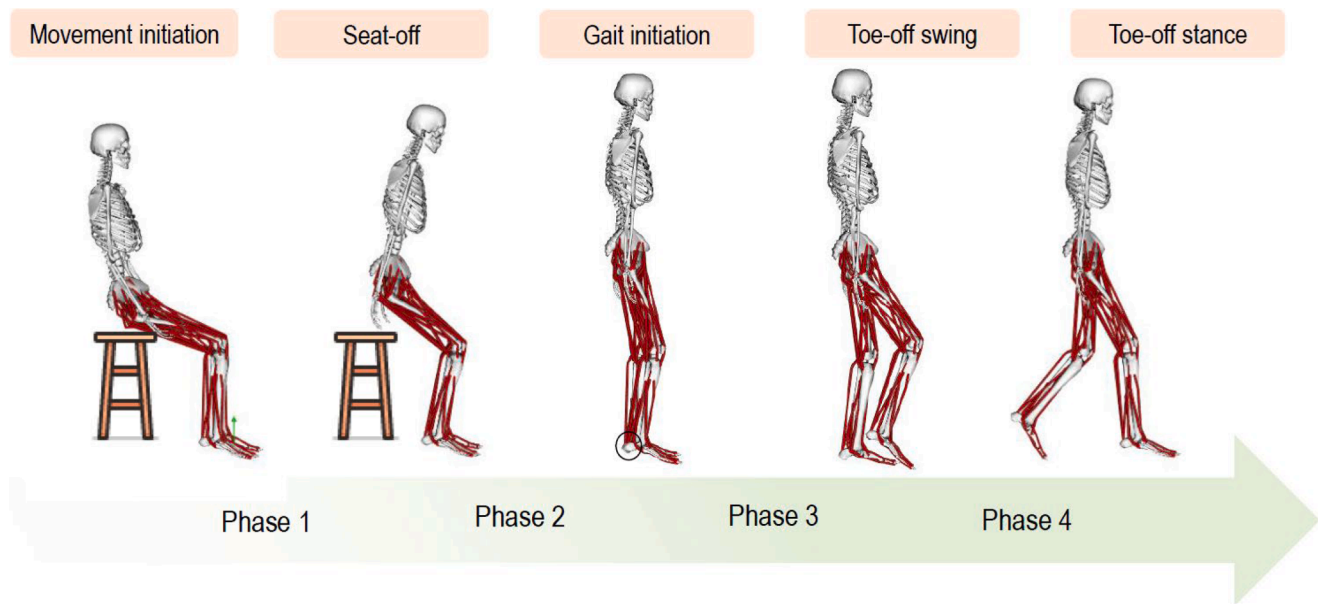


Fig. 3. Phases of STW cycle.

capture and force plate data were utilized to calculate joint angles, joint moments, and MTU kinematics (moment arms and lengths) using the inverse kinematics (IK), inverse dynamics (ID), and muscle analysis tools, respectively, in Opensim. Joint moments from ID are termed 'experimental' and serve as the study's ground truth.

These MTU kinematics, along with normalized EMG data, were then input into the Calibrated EMG-Informed Neuromusculoskeletal Modeling toolbox (CEINMS) to estimate muscle forces for all 40 MTUs of the stepping leg [36]. The stepping leg in STW is the leg that steps out first during the transition from sitting to walking (demonstrated in Section 2.7). The estimation began by mapping measured EMG data from the eight muscles to eleven MTUs [50], assuming that MTUs controlled by the same nerves share similar excitation patterns. A detailed muscle mapping and synthesis list is available in Appendix A (Table A.1).

To account for muscle strength variations, the maximum isometric force for all MTUs was personalized for each subject. The calibration step in the CEINMS toolbox refined it by applying a "strength coefficient", a multiplicative factor for maximum isometric force (ranging from 0.5 to 2.5). This approach reduced the number of parameters to calibrate by grouping muscles with similar characteristics, ensuring participant-specific muscle strength was accurately represented. For muscles without experimental EMG data, the strength coefficient was iteratively adjusted during the execution step of CEINMS to minimize discrepancies between the ground truth and predicted model moments.

The model calibration is done using normalized EMG data, joint moments, and MTU kinematics derived from each participant in two out of five STW trials performed, with the remaining three trials used to estimate muscle forces. This calibration step adjusts the subject-specific MTU parameters (optimal fiber length, tendon slack length, and maximum isometric force) in the scaled MSK model (Table A.2). By aligning the model with actual movement dynamics, it enhances the reliability of muscle force estimates, addressing limitations of methods that rely solely on optimization [30,51].

The EMG-assisted algorithm estimated muscle forces for all 40 MTUs of the stepping leg by synthesizing excitations for muscles not measurable by sEMG while minimally adjusting the EMG data and accurately tracking joint moments. For muscles without EMG data, the excitation patterns of muscles with EMG data provide constraints during optimization, ensuring more physiologically realistic force estimations [52]. The complete modeling workflow is shown in Fig. 2.

2.6. Verification and validation

Direct validation of muscle forces is challenging due to a lack of in vivo data [53]. Despite this limitation, the experimental data, including motion capture and sEMG signals, were successfully validated [54], and joint angles and torques (from ID) aligned well in overall time-varying trends and ranges with previous STW studies [10,55].

The EMG-informed model was validated by assessing whether the predicted joint moments (calculated as muscle forces \times moment arms) accurately tracked the experimental joint moments (from ID) [56,57]. Predicted joint moments closely matched experimental joint moments, with a maximum normalized root-mean-square error (NRMSE) of 0.12 and a minimum Spearman's correlation coefficient (ρ) of 0.84 across five degrees of freedom: hip flexion, internal rotation, adduction, knee flexion, and ankle dorsiflexion (Appendix B, Table B.1). Fig. 4 showed a reasonable match between mean experimental and muscle-predicted joint moments across three age groups during STW. These results are consistent with previous EMG-assisted modeling studies for walking [53, 58].

Additionally, to ensure estimated muscle force values are realistic, average values (derived from GLMM estimated means) were compared with a previous STS study [21]. This study reported a minimum required range of 35.3–49.2 N/kg for the total force of hip and knee extensors. Since the STS study focused on a different task, the comparison was limited to phase 1 (rising) of STW in this study. In all age-sex subgroups, the total required force for hip and knee extensors exceeded this range, supporting the physiological validity of the CEINMS estimates (Appendix B, Table B.2).

Furthermore, the estimated muscle force trends (Figs C.1–C.6, Appendix C) were compared with their expected functional roles, as reflected in joint moments (Fig. 4) during each STW phase, confirming the physiological plausibility of the model. During the rising phases, hip and knee extensors (*gluteus maximus*, *medius*, and *vasti*) exhibited increased forces, peaking at seat-off, corresponding to the hip and knee extension torque peaks. Similarly, *adductor magnus* forces peaked with peak hip adduction torque, aligning with its primary role. In contrast, hip and knee flexors (*rectus femoris*, *iliopsoas*, *add long*) decreased during rising but increased in the stepping phase, corresponding to rising hip and knee flexion torques for swing leg lift and gait initiation. *Dorsiflexors* increased during stepping (phase 4), aligning with dorsiflexion torque. These phase-specific muscle force patterns across age-sex subgroups

Table 2
Definition of STW phases.

	Rising phase		Stepping phase	
	Phase 1 Flexion momentum	Phase 2 Extension	Phase 3 Unloading	Phase 4 Stance
Start event	Movement initiation	Seat-off	Gait initiation (GI)	Swing toe-off
End event	Seat-off	Gait initiation (GI)	Swing toe-off	Stance toe-off
Definition	Begins with the first detectable shift in vertical force (>2 SD) and ends at peak vertical ground reaction force (GRF) during seat-off.	Characterized by the extension of lower limb joints as the body rises, ending at gait initiation (heel off of the swing foot)	Begins as the swing leg heel lifts and concludes when the swing leg completely leaves the force plate.	Ends when the stance foot lifts off, leaving the swing foot flat on the force plate.

validate the model's reliability in capturing realistic muscle recruitment strategies.

2.7. STW phases

The estimated muscle forces were segmented into four phases of STW motion (Fig. 3), as outlined in the literature (Table 2) [59,60]. To ensure consistency across age-sex subgroups, the STW cycle was time-normalized for each group, with phase durations found to be similar across these subgroups (Table D.1, Appendix D). Stepping leg for every trial was determined by referring to the motion capture data during phase 3 of STW.

3. Outcome variables

The variables of interest were the estimated lower limb muscle forces produced during the STW motion, categorized by their functional groups (Appendix E, Table E.1). Fig. 5 illustrates the anatomical location of these muscle groups. Continuous time-series data from all individual trials for each subject was used to capture the variability in muscle forces, ensuring a precise representation of muscle force patterns across the dynamic phases of the task. Averaging the data would have masked this variability, which is crucial for understanding muscle coordination during each phase of the STW motion.

4. Statistical analyses

Statistical analyses were performed to assess age-related variations in muscle forces across age-sex subgroups during STW phases. The Shapiro-Wilk test ($p > 0.05$) and Q-Q plots revealed that muscle force profiles were non-normal and positively skewed. As such, a Generalized Linear Mixed Modeling (GLMM) approach was used to explore these variations. This approach particularly accounted for the hierarchical structure of the data: STW phases nested within trials, trials nested within individuals, and individuals grouped by age (highest level) (Fig. F.1, Appendix F). This modeling framework also addressed the repeated measures design common in biomechanics research, where each participant performed five STW trials.

Repeated measurements (trials) from the same subject are correlated observations, violating the assumption of independence required by many statistical methods. A common practice in such cases is aggregating data across trials by calculating an average for each participant. However, this method overlooks within-subject variability and trial-to-trial muscle force differences, leading to potential biases and reduced statistical power [61]. By contrast, GLMM incorporates all repeated

measurements while explicitly accounting for their correlation, providing a more accurate and comprehensive analysis. This allowed for a robust evaluation of the study hypothesis, capturing both individual-level and group-level patterns while preserving the structure and variability of the data.

GLMM provides a flexible framework for analyzing non-normal data by incorporating fixed and random effects. Fixed effects estimate the average effect of the predictors (age groups) across the population, while random effects capture individual-level variability. Separate GLMMs were developed for each muscle group using a Gamma distribution with a log link function. The Gamma distribution is ideal for modeling continuous, positive-valued data, while the log link function ensures predictions remain positive and addresses the data's skewness [62]. Individual participants were treated as random effects (covariance type = variance components), while the age group was modeled as a fixed effect (Model 1). This allowed the model to focus on the average effect of age groups while accounting for the variability among individual participants. To explore sex-related differences in muscle forces, a second model (Model 2) included an interaction term between age group and sex (sex \times age group) as an additional fixed effect. This term examined how age-related changes in muscle force differed between males and females.

To account for repeated measures, two covariance structures were tested: 1) Diagonal (independent): assumes no correlation between trials and 2) AR1 (first-order autoregressive): assumes each trial is correlated with the previous one, with the correlation diminishing over time. The AR1 structure, selected for its lower AIC and better residual normality, effectively captured correlations between adjacent trials, improving model accuracy. Statistical significance was set at $\alpha = 0.05$. Pairwise contrasts with Sidak correction were used to adjust for multiple comparisons and minimize Type I errors. Analyses were conducted using SPSS Statistics v28 (IBM Corp., New York, US).

5. Results

5.1. Muscle force variations across age-sex subgroups

The estimated means from the GLMM analysis represent the average muscle force during STW, accounting for fixed effects (age group) and random effects (individual variability and repeated measures). These estimates provide a robust measure of muscle force, with higher values indicating greater force production and highlighting each muscle's role across phases. Heat maps (Fig. 6) illustrate variations in muscle forces across age groups (young, middle-aged, older) and sexes (females, males) during different STW phases based on these estimated means.

As illustrated in Fig. 6, the primary knee extensor (*vasti*) and hip extensor (*gluteus maximus*) generate the highest forces during the rising phases (phases 1 and 2), followed by the hip abductor (*gluteus medius*), plantarflexor (*soleus*), and *dorsiflexors* across all age-sex subgroups. As gait began during the stepping phases (phases 3 and 4), the *vasti* muscle group remains dominant in younger and middle-aged adults, followed by *gluteus medius*. However, older males show a shift in muscle force dominance, with higher forces in the *gluteus medius* compared to other age groups (phase 4). Knee flexors (*hamstrings*, *biceps femoris short head*), *dorsiflexors*, plantarflexors (excluding *soleus*), and hip flexors (*iliopsoas*, *addlong*) peak in phase 4 when the stepping leg supports the body's weight. This pattern is observed in males across all age groups, while in older females, it is limited to the *biceps femoris short head*, *gastrocnemius*, and *iliopsoas*.

Muscles such as the *TFL* and *sartorius* generated average forces below 150 N across all phases, indicating their minimal role in STW. In contrast, key muscles like the *vasti*, *gluteus maximus*, *gluteus medius*, *dorsiflexors*, and *soleus* consistently produced higher forces across all age-sex subgroups, highlighting their crucial role in the successful transition from sitting to walking. Henceforth, these muscles will be referred to as the primary STW muscles.

Table 3
Muscle groups showing significant age-related variations during STW phases.

STW phase	Muscle groups with significant variations across age groups	
Phase 1	Function	Muscles
	Hip extensors	<i>gluteus maximus, addmag hamstrings</i>
	Knee extensors	<i>vasti</i>
	Dorsi flexors	<i>tibialis anterior, extensor hallucis longus, extensor digitorum longus</i>
	Plantarflexor	<i>gastrocnemius</i>
Phase 2	Foot plantarflexors	<i>fhl, fdl, tib post</i>
	Plantarflexor	<i>Soleus</i>
	Knee flexor	<i>bfsh</i>
	Hip extensors	<i>gluteus maximus, addmag</i>
	Knee extensors	<i>vasti, rectus femoris</i>
Phase 3	Dorsi flexors	<i>tibialis anterior, extensor hallucis longus, extensor digitorum longus</i>
	Plantarflexor	<i>gastrocnemius</i>
	Hip Adductors	<i>addlong</i>
	Foot plantarflexors	<i>fhl, fdl, tib post</i>
	Dorsi flexors	<i>tibant, edl, ehl</i>
Phase 4	Plantarflexors	<i>soleus, flexor hallucis longus, flexor digitorum longus, tibialis posterior</i>
	Plantarflexors	<i>gastrocnemius</i>
	Foot evertor	<i>perlong</i>
	Hip Adductors	<i>addlong, addmag</i>
	Dorsi flexors	<i>tibialis anterior, extensor hallucis longus, extensor digitorum longus</i>
	Hip Flexors/Knee Extensors	<i>rectus femoris</i>
	Foot evertor	<i>perlong</i>
	Knee flexor/Plantarflexor	<i>gastrocnemius</i>

5.2. Statistical significance of muscle force profiles during different phases of STW

GLMM results are presented as contrast estimates (CE) in Newtons (N), standard errors (SE), and p-values to indicate the magnitude, variability, and statistical significance of the findings. Full statistical details are provided in the supplementary material. Muscle groups not mentioned showed no statistically significant differences across age-sex subgroups, indicating similar force production during STW.

5.2.1. Variation across age groups

A. Phase 1 (movement initiation to seat-off):

Older adults exhibited significantly lower muscle forces for hip extensors – *gluteus maximus, hamstrings*, and *addmag* group, knee extensor – *vasti*, plantarflexors – *gastrocnemius, foot plantarflexors*, and *soleus, dorsiflexors* and knee flexor – *bfsh* compared to young and middle-aged adults ($p < 0.05$ for all pairwise comparisons; see Table S1 for details). Younger and middle-aged adults produced statistically similar muscle forces in phase 1 for most muscle groups, except for the highest *hamstring* forces in younger adults and *foot plantarflexor* forces in middle-aged adults.

B. Phase 2 (seat-off to gait initiation):

During the extension phase, older adults continued to exhibit significantly lower forces in the hip and knee extensors (*gluteus maximus, vasti*, and *rectus femoris*) and *dorsiflexors* (all $p < 0.05$; see Tables S3 and S4). However, their *gastrocnemius* and *foot plantarflexor* forces were comparable to younger adults ($p > 0.05$) while showing higher forces in

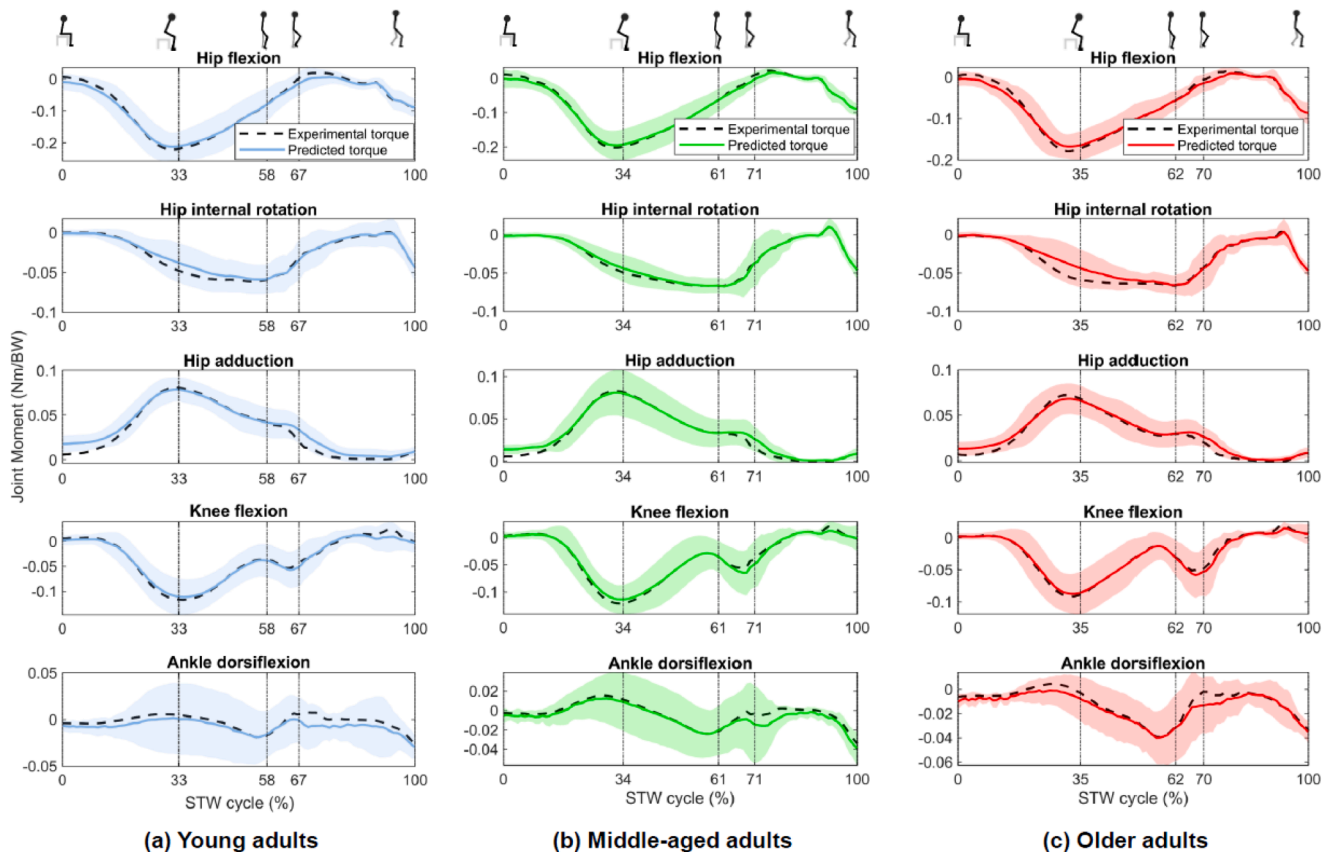


Fig. 4. Mean experimental and predicted torques for hip, knee, and ankle joints in (a) young, (b) middle-aged, and (c) older adults. Shaded regions show one standard deviation of predicted moments. Positive values are defined by subplot titles. Vertical lines mark STW events.

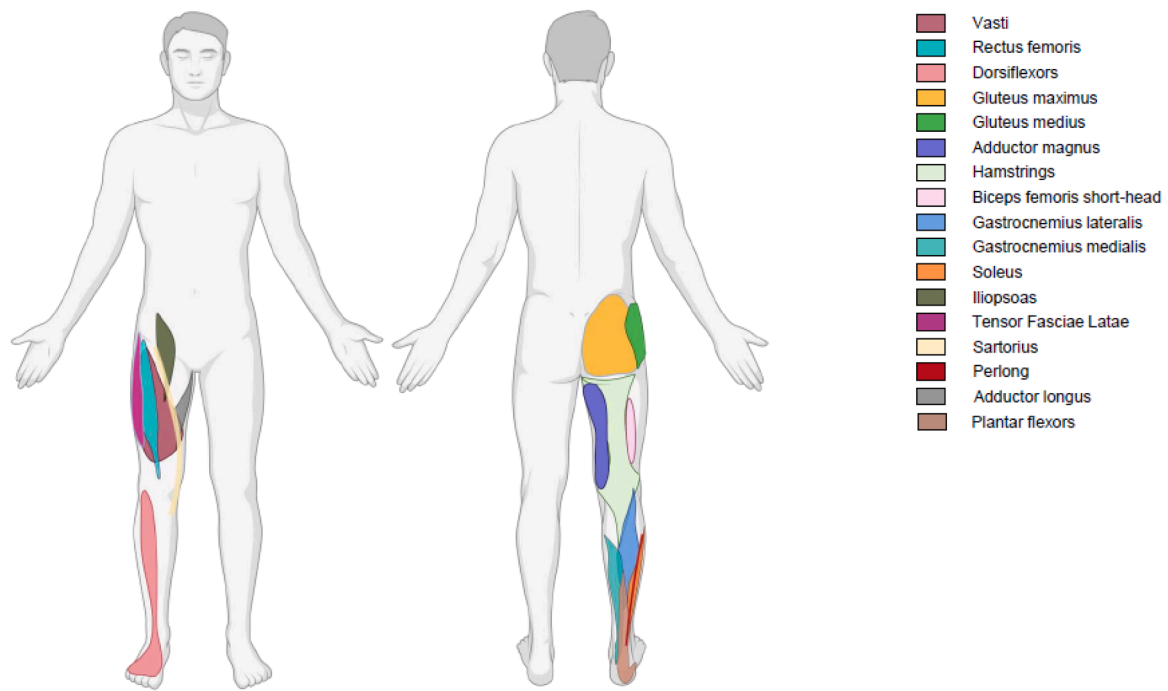


Fig. 5. Illustration of the lower limb muscle groups, with each region color-coded to show anatomical locations (created in BioRender.com).

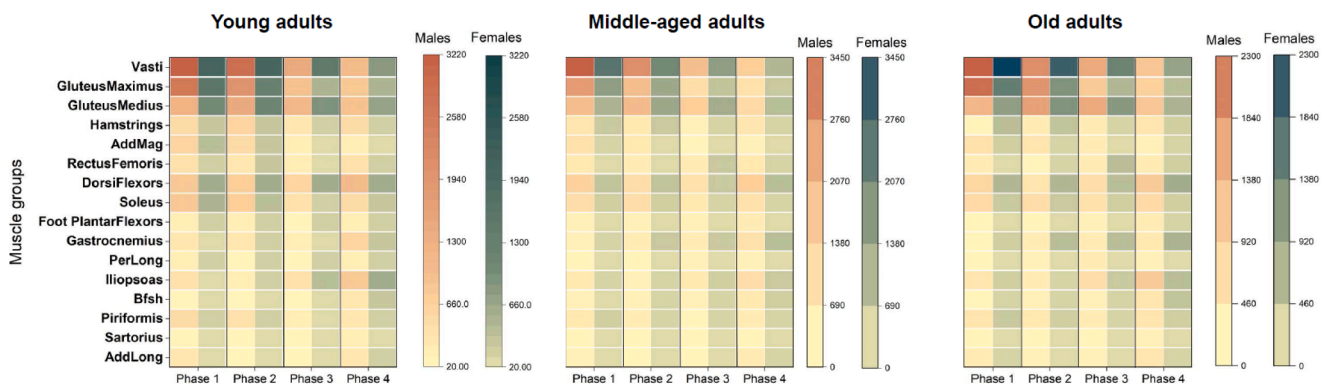


Fig. 6. Heat maps illustrating the estimated mean muscle forces (in Newtons) for males and females across three age groups during different phases of STW. Each age group has a distinct color bar scale, highlighting differences in force production ranges.

the *addlong* group ($p = 0.012$) as compared to middle-aged adults. Younger and middle-aged adults showed statistically similar muscle forces in phase 2, except for the *adductor magnus*, where younger adults generated the highest forces ($p = 0.003$), and the *gastrocnemius*, where middle-aged adults produced the highest ($p = 0.011$).

C. Phase 3 (gait-initiation to toe-off swing):

During gait initiation of the stepping phase, older adults demonstrated significantly higher forces in the *foot plantarflexors* (middle-aged: coefficient = 1.870, $p < 0.001$), *perlong group* (middle-aged: coefficient = 1.356, $p = 0.008$), and *soleus* (younger: coefficient = 0.659, $p = 0.030$; middle-aged: coefficient = 0.770, $p = 0.013$) compared to younger and middle-aged adults. In contrast, older adults demonstrated lower *dorsi-flexor* forces than younger (CE: -244.906 N, $p = 0.009$) and middle-aged adults (CE: -179.419 N, $p = 0.072$).

For other muscles, younger and older adults exhibited statistically similar forces in the *addmag group*, *foot plantarflexors*, *gastrocnemius*, and *perlong group* ($p > 0.05$). Middle-aged adults had the lowest forces for hip adductors (*addlong* and *addmag* groups, $p < 0.05$) but demonstrated the

highest forces for the *gastrocnemius* ($p < 0.01$).

D. Phase 4 (toe-off swing to toe-off stance):

Older adults exhibited significantly lower forces in the ankle plantarflexor/knee flexor (*gastrocnemius* and *biceps femoris short head*), hip flexor/knee extensor (*rectus femoris*), foot evtor (*perlong group*), and *dorsiflexors* compared to younger and middle-aged adults. Among younger and middle-aged adults, muscle forces were similar, except for the *gastrocnemius*, *biceps femoris short head*, and *soleus*, where middle-aged adults showed the highest forces. The majority of muscle groups, however, did not show any variation between age groups.

Table 3 summarizes statistically significant muscle force variations across age groups during different STW phases.

5.2.2. Sex-specific variations across age groups

Fig. 7 presents the statistically significant muscle groups among males and females during different phases of the STW motion.

A. Phase 1 (movement initiation to seat-off):

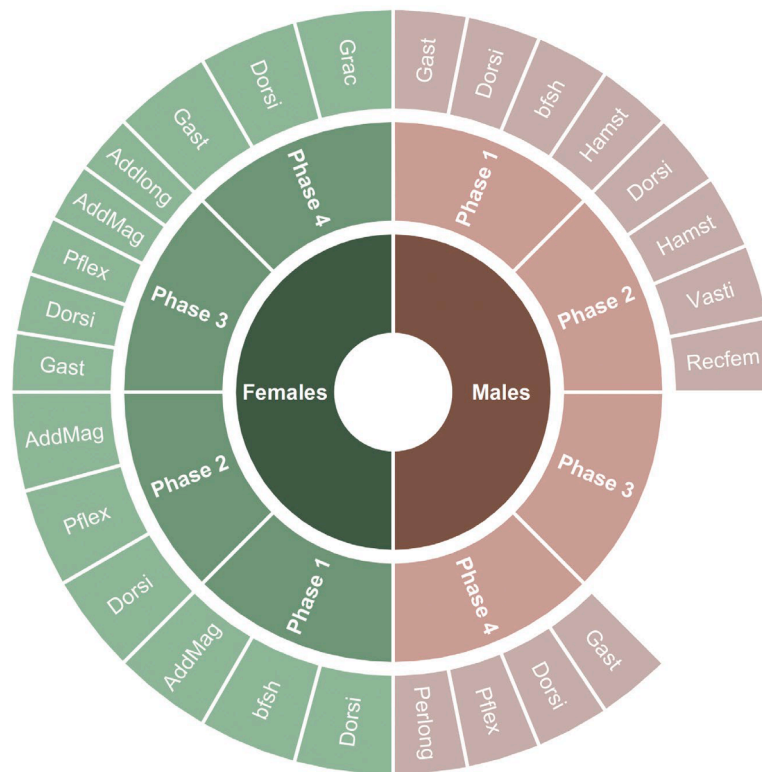


Fig. 7. Statistically significant muscle groups showing sex-based variations during different STW phases. The innermost ring represents the sex of the participants (males and females). The middle ring corresponds to the four phases of the STW, and the outermost ring highlights the specific muscle groups that exhibit significant differences in each phase. Muscle labels are abbreviated as follows: Hamst – hamstrings, AddMag – Adductor Magnus, RecFem – Rectus Femoris, AddLong – Adductor Longus, Gast – Gastrocnemius, Bfsh – Biceps Femoris Short Head, Dorsi – Dorsiflexors, and PIFlex – Foot Plantarflexors.

Older males exhibited the lowest *hamstring* forces compared to both younger (CE: -408.459 N, $p < 0.001$) and middle-aged men (CE: -416.029 N, $p < 0.001$). Interestingly, older women demonstrated higher *hamstring* forces than older men (coefficient: 1.613 , $p < 0.001$). Additionally, older males had lower *gastrocnemius* forces than both younger (CE: -192.096 N, $p = 0.006$) and middle-aged adults (CE: -109.619 N, $p = 0.100$). While older men showed reduced *vasti* muscle forces compared to both younger (CE: -913.922 N) and middle-aged men (CE: -1149.165 N), these differences were not statistically significant, likely due to the small sample size.

Significant age-based variations in *dorsiflexor* and *bfsh* forces were observed in both sexes. For *dorsiflexors*, middle-aged men had higher forces than older men (CE: 418.713 N, $p = 0.013$) and younger men (CE: 257.304 N, $p = 0.090$). Younger females had significantly higher *dorsiflexor* forces than older females (CE: 391.113 N, $p = 0.004$). In *bfsh*, older males had lower forces than younger males ($p < 0.001$), while older females had the lowest forces as compared to younger ($p = 0.042$) and middle-aged females ($p = 0.042$). Younger females also had significantly higher *addmag* forces.

B. Phase 2 (seat-off to gait initiation):

In the knee extensor muscles (*vasti* and *rectus femoris*), older males demonstrated lower forces compared to both younger ($p < 0.001$) and middle-aged men ($p < 0.001$), while females showed no significant differences. Additionally, older men also had the lowest hamstring forces compared to other age groups ($p < 0.05$).

Females showed significant variations in *addmag*, *foot plantarflexor* and *dorsiflexor* forces across age groups while men showed no significant variations in these groups except *dorsiflexors*. Both older males and females produced lowest *dorsiflexor* forces across age groups. However, older women had higher forces in *foot plantarflexors* than middle-aged

women and comparable forces to younger females.

C. Phase 3 (gait-initiation to toe-off swing):

Males showed no significant age-related differences in muscle forces, although older males tended to have higher *gluteus medius* forces compared to middle-aged (CE: 144.364 N, $p > 0.05$) and younger males (CE: 232.427 N, $p > 0.05$); however, these differences were not statistically significant.

In contrast, females exhibited significant age-related variations in several muscle groups. Middle-aged females had the lowest forces in hip adductors (*addlong* and *addmag* groups, $p < 0.05$), foot plantarflexors and the highest forces in the *gastrocnemius* ($p < 0.01$). Younger and older females displayed statistically similar forces in the *addmag* group, *foot plantarflexors*, and *gastrocnemius* ($p > 0.05$). Older females tended to have higher *soleus* forces than middle-aged (CE: 223.026 N, $p = 0.067$) and younger females (CE: 200.299 N, $p = 0.084$), but these differences were not statistically significant. Younger females had significantly higher *dorsiflexor* forces than older females (CE: 364.724 N, $p = 0.006$), while middle-aged and older females showed no difference.

D. Phase 4 (toe-off swing to toe-off stance):

Sex-based variations across age groups were limited to ankle muscles. Older adults, both males and females, showed the lowest *dorsiflexor* and *gastrocnemius* forces. Males also exhibited variations in *foot plantarflexors*, with middle-aged men showing the highest *dorsiflexor*, *foot plantarflexor*, and *perlong* group forces, while middle-aged females had the highest *gastrocnemius* forces. Older males had higher *gluteus medius* forces than other age groups, though not statistically significant. In most muscle groups, males had significantly higher forces than females.

6. Discussion

The present research assessed the lower limb muscle force variations in males and females across age groups during the STW motion. Since direct measurement of muscle forces is not feasible [19], EMG-informed methods offer improved accuracy in estimating muscle forces. This method enabled detailed analysis of lower limb muscles (both surface and deep) for a successful STW performance. The reliability of these estimations was confirmed through comparisons with a previous STS study, experimental joint moments, expected muscle roles, and experimental data quality.

GLMM results revealed significant age- & sex-related variations in muscle forces during different phases of STW, supporting the study's first hypothesis. While phase durations were similar across age groups, aligning with past literature [20,22], muscle force variations were phase-specific. Notably, primary STW muscles, except the *gluteus medius*, exhibited age-related variations during the rising phases. Older adults consistently demonstrated lower forces in all primary STW muscles during rising (except for the *soleus*), emphasizing the need for targeted strengthening of these muscle groups. Additionally, middle-aged adults generated the highest *gastrocnemius* forces (phases 2–4) and lowest hip adductor forces during gait initiation, highlighting early signs of functional decline.

Significant variations in ankle-spanning muscles were observed during the stepping phases, particularly among older adults. Older females, in particular, generated significantly higher forces in the plantarflexors and evertors (excluding the *gastrocnemius*) as gait initiation began. This shift suggests a compensatory mechanism, promoting plantarflexion to support the forward propulsion of the stepping leg. The increased ankle plantarflexion moment in older adults, compared to the dorsiflexion moment observed in other age groups, further reflects this adaptation, enabling effective gait transitions (Fig. 4). This supports the critical role of ankle plantarflexor [63,64] and evertor muscles in gait initiation and suggest that preserving these muscle groups is vital to maintain mobility with age.

Sex-based variations across age groups were generally absent in primary STW muscles, except for *dorsiflexors*. However, as hypothesized, notable sex differences emerged in specific muscle groups. Interestingly, during gait initiation (phase 3), middle-aged females exhibited the lowest *hip adductor* and highest *gastrocnemius* forces, while males showed no significant age-related differences. This indicates a greater vulnerability in females to muscle function decline [65] and fall risks with aging, particularly during gait initiation [66,67]. Older males, meanwhile, exhibited higher *gluteus medius* forces during stepping phases. However, this finding was not statistically significant, likely due to the small sample size, highlighting the need for further research.

Contrary to the study's second hypothesis that age-related variations in muscle forces would lead to altered recruitment strategies across phases, the key findings identified consistent primary STW muscles involved in lower limb recruitment across all age-sex subgroups. The *vasti*, *gluteus maximus*, *gluteus medius*, *dorsiflexors*, and *soleus*, generated the highest average muscle forces, aligning with a previous study on STS [22]. These muscles, except *dorsiflexors*, exhibited the highest forces during the rising phases (phases 1 and 2), emphasizing their essential role in elevating the body's center of mass (COM) during rising. These results indicate that overall muscle recruitment strategies remain consistent across age-sex subgroups in healthy aging during STW.

These results highlight that compensation in healthy aging involves variations in muscle force production within the same muscle groups rather than altered muscle recruitment strategies to maintain task performance. Altered recruitment may arise in individuals with movement disorders or pathological conditions, warranting further research. Despite reduced muscle forces in primary STW muscles during rising phases, older adults maintained similar STW phase durations compared to other age groups. This was compensated by increasing forces in ankle plantarflexor muscles (except *gastrocnemius*) and hip abductors (*gluteus*

medius) to propel the body forward into gait. While this compensation may sustain short-term performance, it could accelerate joint degeneration and mobility challenges as force production declines with age. When this compensation can no longer facilitate the transition to walking, mobility limitations may arise [68]. To mitigate these risks, interventions should target strengthening STW muscles starting in middle age, when early signs of functional decline, such as greater reliance on the *gastrocnemius* and weaker hip adductor muscles, become evident.

Middle-aged adults were also included to explore early signs of muscle function decline, which typically begins in the third decade of life [69,70]. Targeted interventions, like muscle coordination retraining, could help redistribute force production to other plantarflexor muscles, like the *soleus*, to reduce knee load and injury risk [71]. For middle-aged females, exercise programs such as Tai Chi enhance dynamic stability during gait initiation [66,72]. Future research should explore how these muscle force variations contribute to lower limb joint loadings, offering valuable insights into muscle and joint preservation in healthy aging. Additionally, exploring the relationship between muscle force variations and STW movement strategies in healthy aging could provide deeper insights into muscle function and mobility.

Some limitations of this study should be acknowledged. The uneven sex distribution in the study may limit the generalizability of the findings, restricting definitive conclusions. Despite this, the findings provide an initial exploration of sex-based adaptations of muscle forces in healthy aging during STW, emphasizing the need for future research with more balanced participant groups. sEMG was collected from only eight dominant leg muscles, excluding the primary hip muscle (*gluteus maximus*) due to collection constraints. However, the hybrid EMG-informed model offers greater accuracy than static optimization-based models [73,74]. Integrating EMG-calibrated MTU parameters ensures that subject-specific EMG-force relationships are accurately captured [53].

7. Conclusion

The present study establishes a benchmark for muscle force profiles across age-sex subgroups. The findings reveal consistent muscle recruitment strategies with compensatory variations in muscle force production across age groups. These results provide early indicators of functional decline and offer valuable insights for enhancing mobility while preventing further deterioration. Efforts should focus on strengthening primary STW muscles beyond knee extensors, incorporating tailored strategies for specific populations. For example, exercises like Tai Chi, known to enhance dynamic stability during gait initiation, will especially benefit females across age groups. Designing age- and sex-specific, biomechanically-informed lifestyle recommendations can improve mobility and quality of life for individuals with movement impairments.

Abbreviations

ADL	Activities of Daily Living
AIC	Akaike Information Criterion
AR1	First-order AutoRegressive
CAST	Calibrated Anatomical System Technique
CE	Contrast Estimates
CEINMS	Calibrated EMG-Informed Neuromusculoskeletal modeling
COM	Center of Mass
EMG	Electromyography
F	Females
GRF	Ground Reaction Forces
GLMM	Generalized Linear Mixed Modeling
IK	Inverse Kinematics
ID	Inverse dynamics
M	Males
MSK	Musculoskeletal

(continued on next page)

(continued)

MTU	Muscle-Tendon Units
MVC	Maximum voluntary contraction
N	Newton
NMS	Neuromusculoskeletal
NRMSE	Normalized root-mean-square error
sEMG	Surface Electromyography
SE	Standard Errors
SENIAM	Surface Electromyography for the Non-Invasive Assessment of Muscle
STS	Sit-To-Stand
STW	Sit-To-Walk
TUG	Timed Up and Go

CRediT authorship contribution statement

Zakia Hussain: Writing – original draft, Visualization, Validation, Software, Methodology, Investigation, Formal analysis, Conceptualization. **Alpha Agape Gopalai:** Writing – review & editing, Supervision, Resources, Project administration, Funding acquisition, Conceptualization. **Siti Anom Ahmad:** Writing – review & editing. **Mazatulfazura Sf Binti Salim:** Writing – review & editing. **Darwin Gouwanda:** Funding acquisition. **Pei-Lee Teh:** Writing – review & editing.

Declaration of competing interest

The authors declare the following financial interests/personal

Supplementary materials

Supplementary material associated with this article can be found, in the online version, at [doi:10.1016/j.rineng.2025.104660](https://doi.org/10.1016/j.rineng.2025.104660).

APPENDIX A

Muscle groups have been classified according to their primary function: (A) Hip flexors, (B) Hip extensors, (C) Hip adductors, (D) Hip abductors, (E) Knee extensors, (F) Knee flexors, (G) Ankle Dorsiflexors and (H) Ankle Plantar flexors and (I) Evertors

Table A.1
Mapping of lower-limb muscles, corresponding model actuators and excitation inputs*.

Primary Function	Muscle groups	Muscles	Model MTUs/ actuators	Excitation input
A, C	Addlong	Adductor brevis Adductor longus	<i>addbrev</i> <i>addlong</i>	Synthesised Synthesised
B, C	Adductor magnus	Adductor magnus	<i>addmagDist</i> <i>addmagIsch</i> <i>addmagMid</i> <i>addmagProx</i>	Synthesised Synthesised Synthesised Synthesised
G	Dorsiflexors	Extensor digitorum longus Extensor hallucis longus Tibialis anterior	<i>edl</i> <i>ehl</i> <i>tibant</i>	Synthesised Synthesised EMG (Tibialis anterior)
F, H	Gastrocnemius	Lateral gastrocnemius Medial gastrocnemius	<i>gaslat</i> <i>gamed</i>	EMG (Lateral gastrocnemius) EMG (Medial gastrocnemius)
B	Gluteus maximus	Gluteus maximus	<i>g1max1</i> <i>g1max2</i> <i>g1max3</i>	Synthesised Synthesised Synthesised
D	Gluteus medius	Gluteus medius Gluteus minimus	<i>g1med1</i> <i>g1med2</i> <i>g1med3</i> <i>g1min1</i> <i>g1min2</i> <i>g1min3</i>	Synthesised Synthesised Synthesised Synthesised Synthesised Synthesised
A, D B, F	Hamstrings	Tensor fasciae latae Biceps femoris long head	<i>tfl</i> <i>bflh</i>	Synthesised EMG (Biceps femoris long head)
		Semimembranosus Semitendinosus	<i>semimem</i> <i>semiten</i>	EMG (Semitendinosus) EMG (Semitendinosus)
F	Biceps Femoris Short Head	Biceps femoris short head	<i>bflsh</i>	EMG (Biceps femoris long head)
C, F	Gracilis	Gracilis	<i>grac</i>	Synthesised
A	Iliopsoas	Iliacus Psoas major	<i>iliacus</i> <i>psaos</i>	Synthesised Synthesised

(continued on next page)

relationships which may be considered as potential competing interests: Alpha Agape Gopalai reports financial support was provided by Ministry of Higher Education, Malaysia. Darwin Gouwanda reports financial support was provided by Malaysia Ministry of Higher Education. If there are other authors, they declare that they have no known competing financial interests or personal relationships that could have appeared to influence the work reported in this paper.

Data availability

All the experimental data, including marker trajectories, force data, and EMG used in this study are available in the Bridges Repository by Monash University, with the identifier: <https://doi.org/10.26180/24515092.v4>

Acknowledgments

The first author thanks Dr. Tim Powers from the Monash Statistical Consulting Service for his invaluable guidance on generalized linear mixed models (GLMM). This work was supported by the Ministry of Higher Education, Malaysia, under the project numbers FRGS/1/2022/TK07/MUSM/02/2 and FRGS/1/2020/TK0/MUSM/02/2.

Table A.1 (continued)

Primary Function	Muscle groups	Muscles	Model MTUs/ actuators	Excitation input
I	PerLong	Peroneus brevis	<i>perbrev</i>	Synthesised
		Peroneus longus	<i>perlong</i>	Synthesised
H	Plantarflexors	Flexor digitorum longus	<i>fdl</i>	Synthesised
		Flexor hallucis longus	<i>fhf</i>	Synthesised
		Tibialis posterior	<i>tibpost</i>	Synthesised
D	Piriformis	Piriformis	<i>piri</i>	Synthesised
A, E	Rectus femoris	Rectus femoris	<i>recfem</i>	EMG (Rectus femoris)
H	Soleus	Soleus	<i>soleus</i>	Synthesised
E	Vasti	Vastus lateralis	<i>vaslat</i>	EMG (Vastus lateralis)
		Vastus medialis	<i>vasmed</i>	EMG (Vastus medialis)
		Vastus intermedius	<i>vasint</i>	Mean EMG (Vastus lateralis & Vastus medialis)
A, F	Sartorius	Sartorius	<i>sart</i>	Synthesised

* EMG excitations are derived from surface electromyography; Synthesised excitations are constructed using static optimization algorithm.

TABLE A.2
CEINMS calibration configuration information of MTU parameters.

MTU parameter	Initial value	Boundary
C ₁	-0.75	[-0.95 -0.05]
C ₂	-0.75	[-0.95 -0.05]
Shape factor (A)	0.5	[-2.999 -0.001]
Tendon slack length	Calculated for each subject[49]	[95 % - 105 %] of initial value
Optimal fiber length	Calculated for each subject[49]	[95 % - 105 %] of initial value
Strength coefficient	Original Rajagopal model value	[50 % - 150 %] of initial value

APPENDIX B

Table B.1
Averaged NRMSE and Spearman’s correlation coefficients between experimental and predicted joint moments across age groups.

Performance metric	Model performance		
	Young adults	Middle-aged adults	Older adults
NRMSE (Mean±SD)			
Hip flexion	0.06±0.03	0.05±0.03	0.06±0.02
Hip adduction	0.09±0.06	0.07±0.04	0.10±0.09
Hip internal rotation	0.11±0.04	0.09±0.05	0.09±0.03
Knee flexion	0.05±0.04	0.05±0.03	0.05±0.02
Ankle dorsiflexion	0.12±0.05	0.11±0.04	0.08±0.04
Spearman’s correlation coefficient (ρ)			
Hip flexion	0.98±0.02	0.98±0.03	0.98±0.01
Hip adduction	0.93±0.12	0.97±0.03	0.92±0.15
Hip internal rotation	0.95±0.02	0.95±0.04	0.96±0.03
Knee flexion	0.96±0.05	0.98±0.02	0.97±0.02
Ankle dorsiflexion	0.84±0.11	0.82±0.21	0.89±0.13

TABLE B.2
Total average force (N/Kg) of hip and knee extensors across age sex-subgroups.

Age group	Sex	Average body mass (Kg)	Vasti	GMax	Recfem	Hamstrings	Total force
Young	Male	71.65	44.82	36.63	4.86	6.66	92.97
	Female	49.38	42.70	32.01	3.44	6.61	84.75
Middle-aged	Male	77.44	44.50	29.90	5.65	6.26	86.31
	Female	56.71	39.22	23.83	1.29	6.96	71.29
Old	Male	66.59	34.50	32.01	2.44	1.03	69.98
	Female	57.32	32.88	22.50	1.99	6.02	63.40

These values were obtained by dividing estimated means of the muscles by average weight.

$$\text{Average forces} \left(\frac{N}{Kg} \right) = \frac{\text{Estimated means}}{\text{Average body mass}}$$

The estimated means of all muscles are illustrated in heat maps in Fig. 6.

APPENDIX C

Figs C.1–C.6 in this section present the average muscle forces (N) with one standard deviation (SD) for each age-sex subgroup. When mean, ± 1 SD produced negative values; these were clipped to zero to reflect the physiological constraint that muscle forces cannot be negative. Negative values arose in cases of high variability relative to small mean forces, particularly during phases of minimal muscle forces. High standard deviations in some muscle groups indicate variability between individuals, similar to a previous STS study[22] for certain muscles. These variations, however, do not undermine the model’s physiological plausibility.

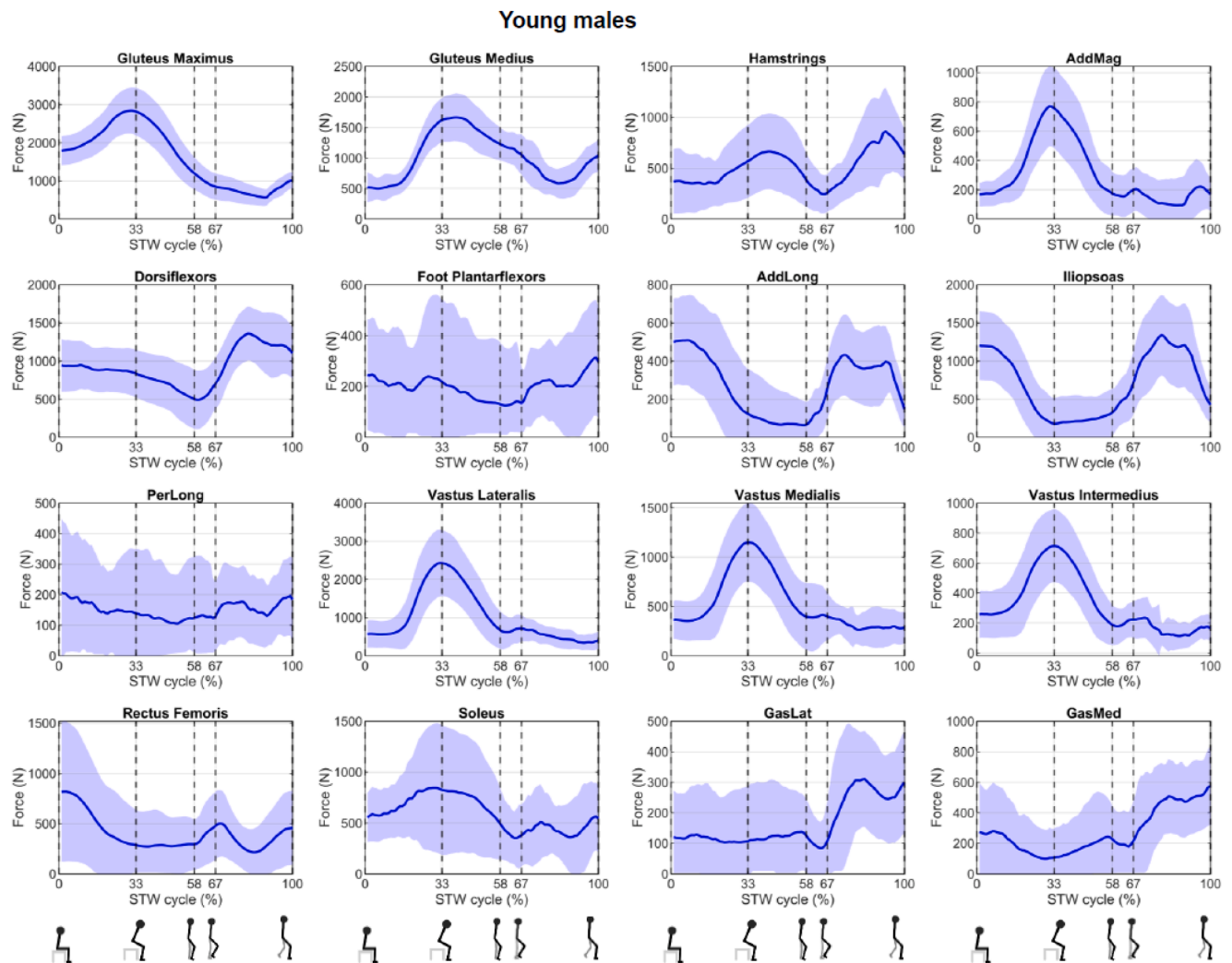


Fig. C.1. Average muscle forces (N) for young males during the STW cycle. The shaded region represents one standard deviation, and vertical lines mark key STW events.

Young females

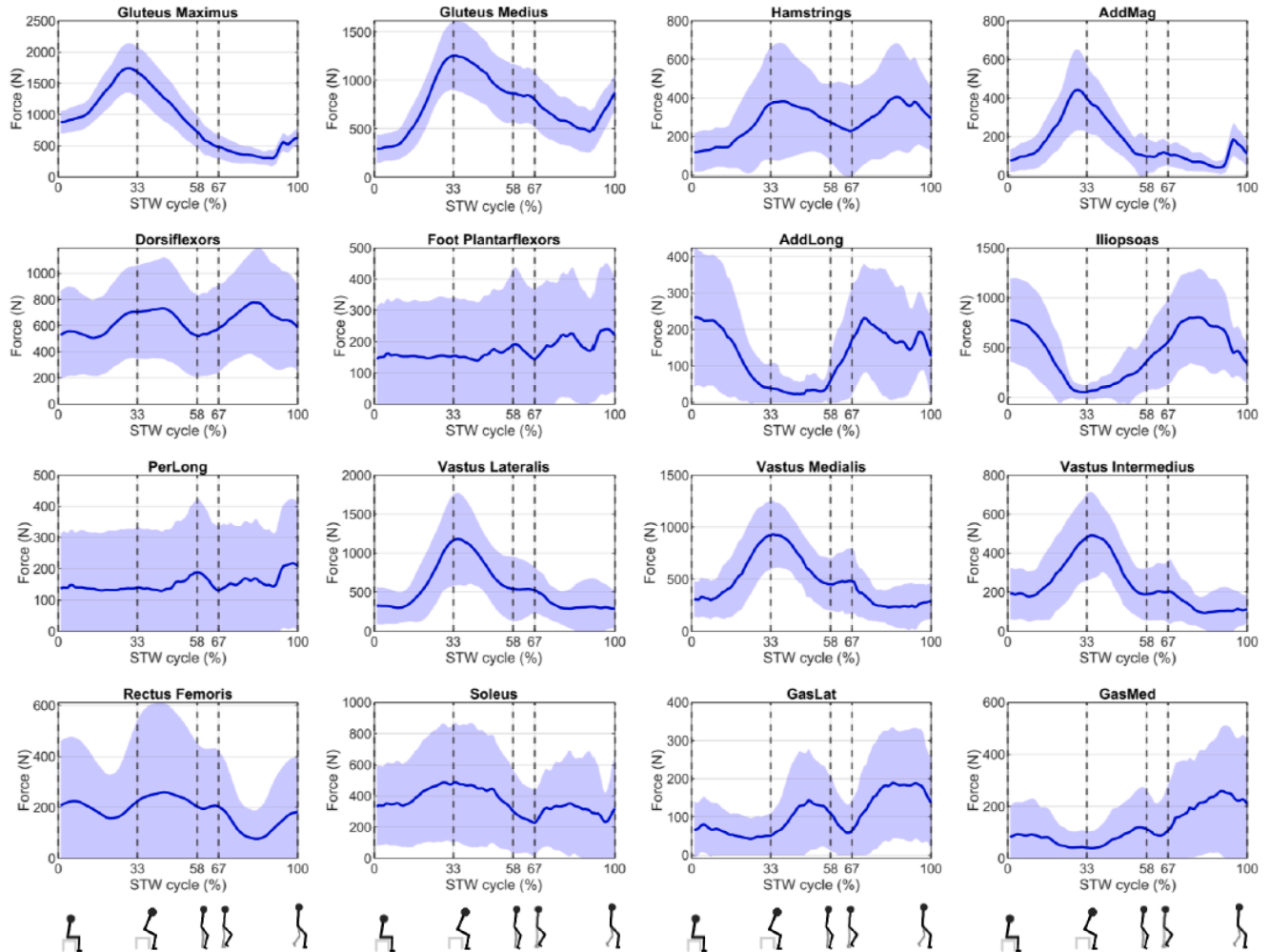


Fig. C.2. Average muscle forces (N) for young females during the STW cycle. The shaded region represents one standard deviation, and vertical lines mark key STW events.

Middle-aged males

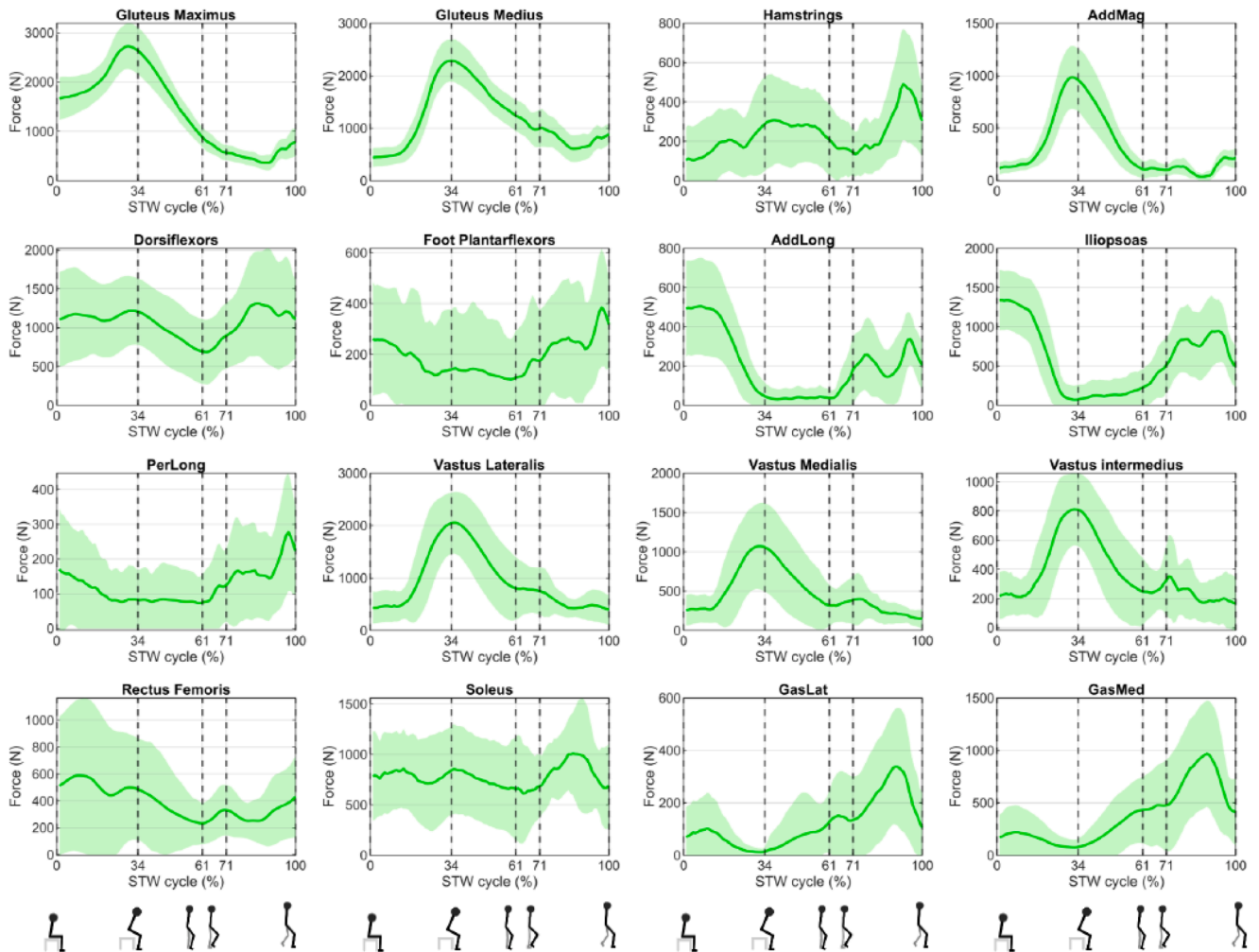


Fig. C.3. Average muscle forces (N) for middle-aged males during the STW cycle. The shaded region represents one standard deviation, and vertical lines mark key STW events.

Middle-aged females

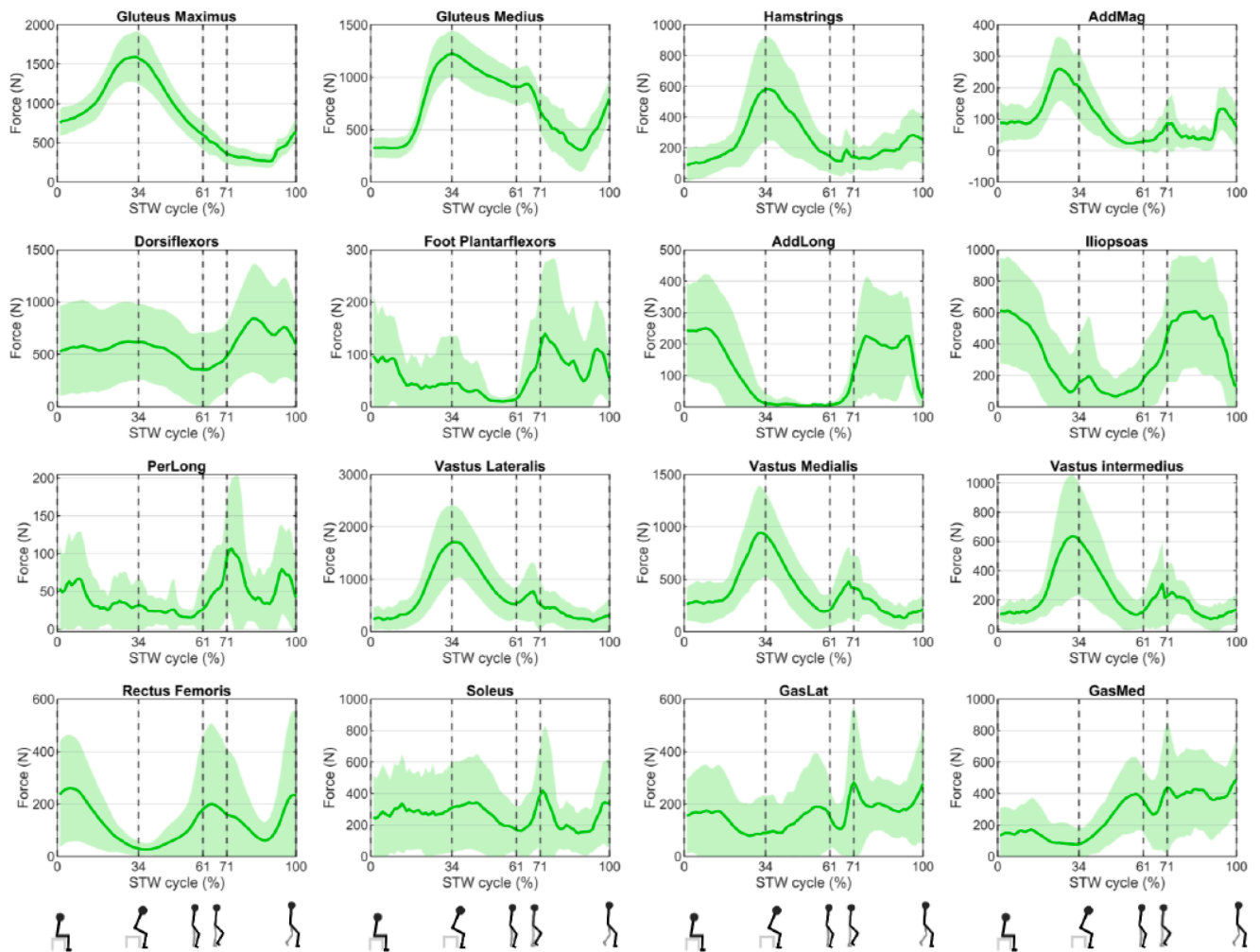


Fig. C.4. Average muscle forces (N) for middle-aged females during the STW cycle. The shaded region represents one standard deviation, and vertical lines mark key STW events.

Old males

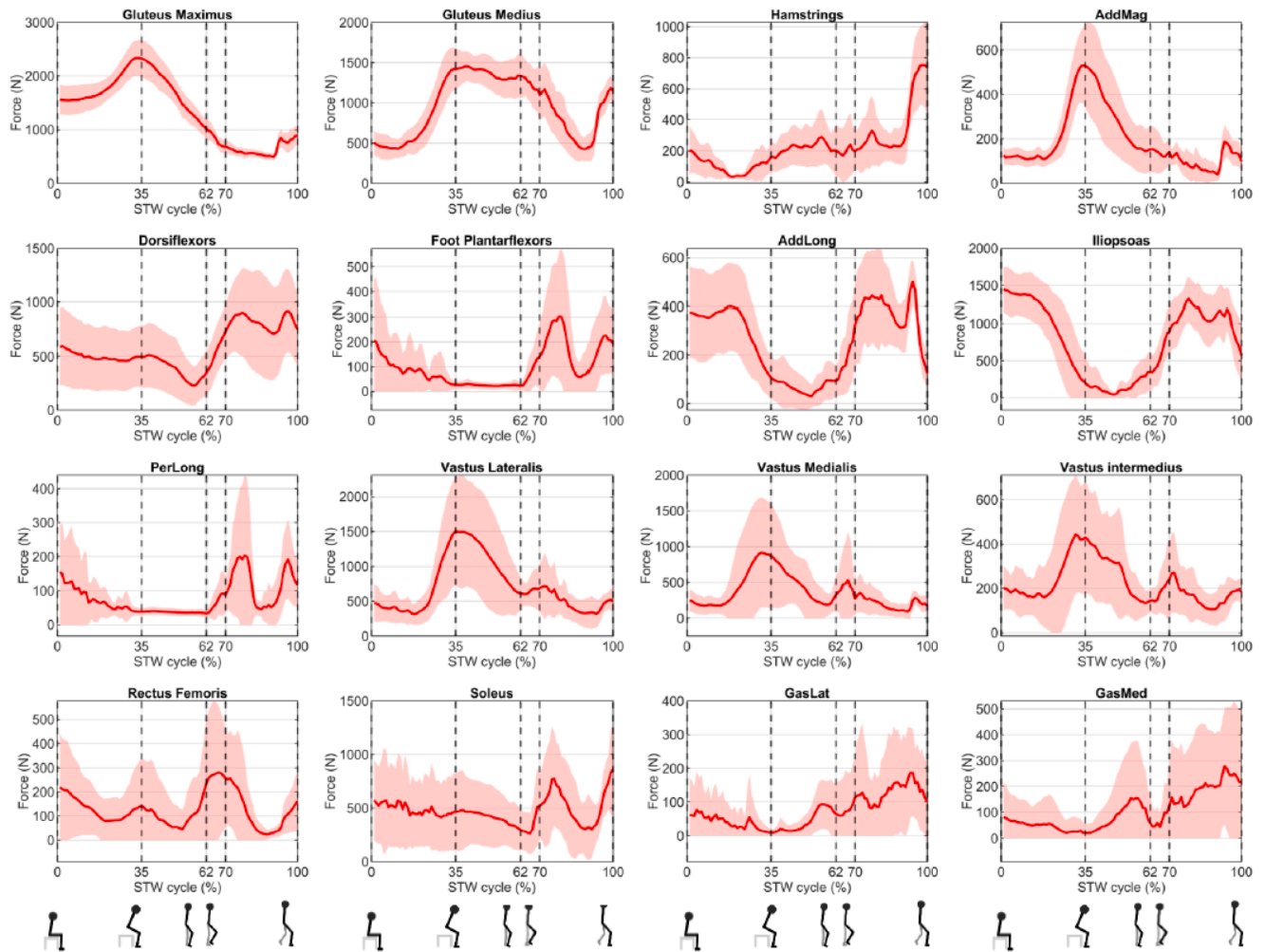


Fig. C.5. Average muscle forces (N) for old males during the STW cycle. The shaded region represents one standard deviation, and vertical lines mark key STW events.

Old females

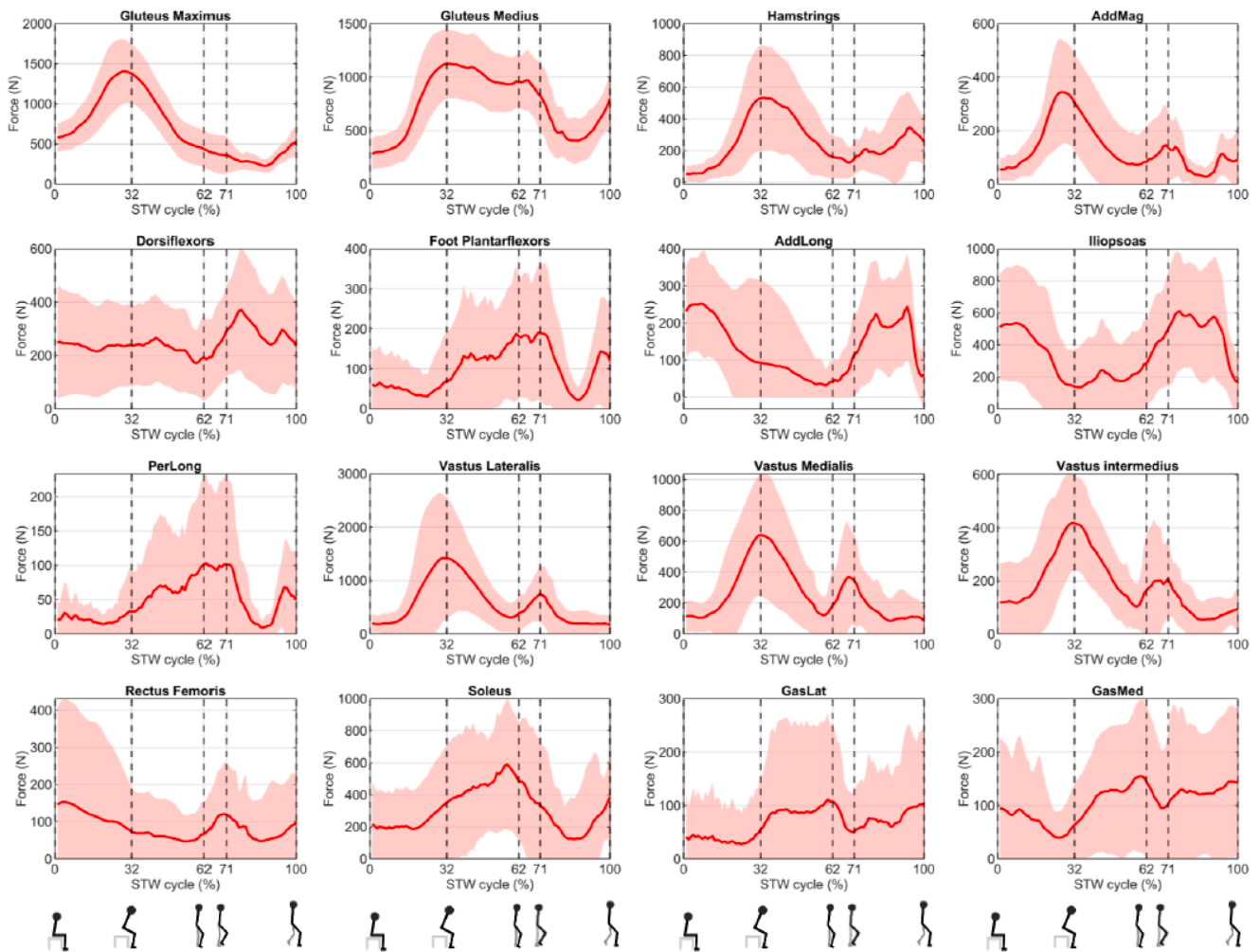


Fig. C.6. Average muscle forces (N) for old females during the STW cycle. The shaded region represents one standard deviation, and vertical lines mark key STW events.

APPENDIX D

Table D.1
Time-normalized event occurrence in STW cycle across all age-sex subgroups.

Age group	Sex	Movement initiation	Seat-off	Gait initiation	Swing toe-off	Stance toe-off
Young	Male	0	33	58	68	100
	Female	0	34	59	67	100
Middle-aged	Male	0	35	62	71	100
	Female	0	34	60	71	100
Old	Male	0	37	62	70	100
	Female	0	32	62	71	100

APPENDIX E

Table E.1
Lower limb muscle groups and functional roles.

No.	Muscle group name	Muscles	Anatomical Functional group
1	Gluteus Maximus	Gluteus Maximus	Hip Extensors
2	Gluteus Medius	Gluteus Medius, Gluteus Minimus	Hip Abductors
3	Hamstrings	Biceps Femoris Long Head, Semitendinosus, Semimembranosus	Hip Extensors/Knee Flexors
4	Biceps Femoris Short Head (bfsH)	Biceps Femoris Short Head	Knee Flexors
5	Vasti	Vastus Lateralis, Vastus Medialis, Vastus Intermedialis	Knee Extensors
6	Rectus Femoris	Rectus Femoris	Hip Flexors/Knee Extensors
7	Addlong	Adductor Longus, Adductor Brevis	Hip Adductors/Hip flexor
8	Adductor Magnus (Addmag)	Adductor Magnus	Hip Adductors/Extensors
9	Gastrocnemius	Gastrocnemius Lateralis, Gastrocnemius Medialis	Plantar Flexors/Knee Flexors
10	Soleus	Soleus	Plantar Flexors
11	Plantarflexors	Flexor Hallucis Longus, Flexor Digitorum Longus, Tibialis Posterior	Plantar Flexors
12	Dorsiflexors	Tibialis Anterior, Extensor Hallucis Longus, Extensor Digitorum Longus	Dorsiflexors
13	Iliopsoas	Psoas, Iliacus	Hip Flexors
14	PerLong	Peroneus Longus, Peroneus Brevis	Evertors
15	Sartorius	Sartorius	Hip Flexors/Knee Flexors
16	Tensor Fasciae Latae (TFL)	Tensor Fasciae Latae	Hip Abductors/Flexors

APPENDIX F

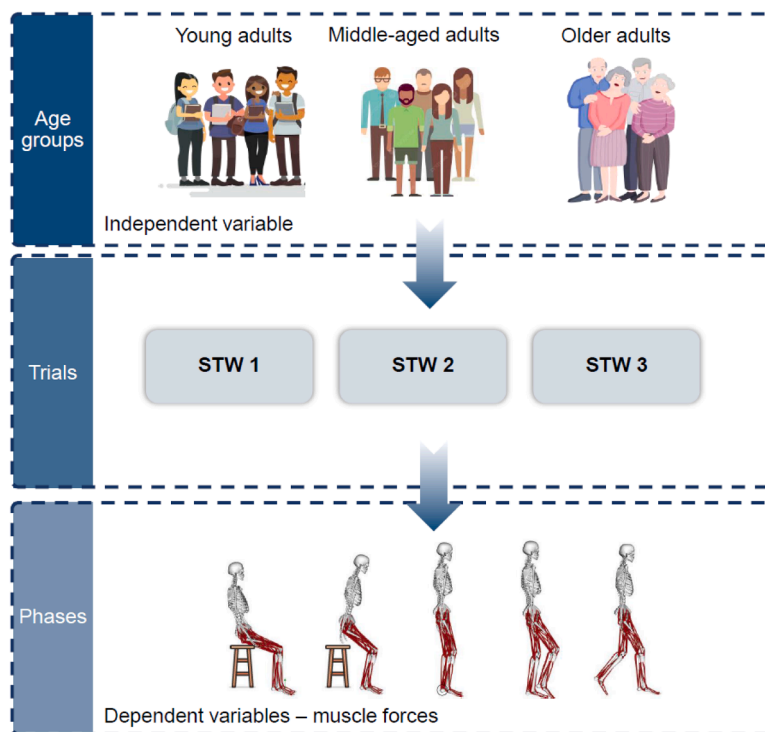


Fig. F.1. Multilevel nested structure of GLMM where the top level is the age group (independent variable), the middle level is the trials, and the last level includes the 4 phases of each STW trial. Every subject performed 3 STW trials (repeated measure). Muscle forces (dependent variable) for each phase of STW were analyzed using GLMM. Individual subject variability was modeled as a random effect, while age groups and age group-sex interaction were modeled as fixed effects.

References

[1] G. Khalili, M. Zargoush, K. Huang, S. Ghazalbash, Exploring trajectories of functional decline and recovery among older adults: a data-driven approach, *Sci. Rep.* 14 (1) (2024) 1–14, <https://doi.org/10.1038/s41598-024-56606-0>.

[2] P. Maresova, O. Krejcar, R. Maskuriy, et al., Challenges and opportunity in mobility among older adults– key determinant identification, *BMC Geriatr.* 23 (1) (2023) 1–29, <https://doi.org/10.1186/s12877-023-04106-7>.

[3] A. Magnan, B.J. McFadyen, G. St-Vincent, Modification of the sit-to-stand task with the addition of gait initiation, *Gait. Posture* 4 (3) (1996) 232–241, [https://doi.org/10.1016/0966-6362\(95\)01048-3](https://doi.org/10.1016/0966-6362(95)01048-3).

[4] A. Kerr, D. Rafferty, K.M. Kerr, B. Durward, Timing phases of the sit-to-walk movement: validity of a clinical test, *Gait. Posture* 26 (1) (2007) 11–16, <https://doi.org/10.1016/j.gaitpost.2006.07.004>.

[5] T. Chen, L.S. Chou, Effects of muscle strength and balance control on sit-to-walk and turn durations in the timed up and go test, *Arch. Phys. Med. Rehabil.* 98 (12) (2017) 2471–2476, <https://doi.org/10.1016/j.apmr.2017.04.003>.

[6] N.B. Alexander, A.B. Schultz, J.A. Ashton-Miller, M.M. Gross, B. Giordani, Muscle strength and rising from a chair in older adults, in: *Muscle and Nerve*, 20, 1997, [https://doi.org/10.1002/\(sici\)1097-4598\(1997\)5+<56::aid-mus14>3.0.co;2-x](https://doi.org/10.1002/(sici)1097-4598(1997)5+<56::aid-mus14>3.0.co;2-x).

[7] S.R. Lord, S.M. Murray, K. Chapman, B. Munro, A. Tiedemann, Sit-to-stand performance depends on sensation, speed, balance, and psychological status in addition to strength in older people, *J. Gerontol. - Biol. Sci. Med. Sci.* 57 (8) (2002), <https://doi.org/10.1093/gerona/57.8.M539>.

- [8] J.C. Mcleod, B.S. Currier, C.V. Lowisz, S.M. Phillips, The influence of resistance exercise training prescription variables on skeletal muscle mass, strength, and physical function in healthy adults: an umbrella review, *J. Sport Health Sci.* 13 (1) (2024) 47–60, <https://doi.org/10.1016/j.jshs.2023.06.005>.
- [9] V.R. Kedlian, Y. Wang, T. Liu, et al., Human skeletal muscle aging atlas, *Nat. Aging* 4 (5) (2024) 727–744, <https://doi.org/10.1038/s43587-024-00613-3>.
- [10] P. Dehail, E. Bestaven, F. Muller, et al., Kinematic and electromyographic analysis of rising from a chair during a “sit-to-walk” task in elderly subjects: role of strength, *Clin. Biomech.* 22 (10) (2007) 1096–1103, <https://doi.org/10.1016/j.clinbiomech.2007.07.015>.
- [11] K.L. Bennell, M. Kyriakides, B. Metcalf, et al., Neuromuscular versus quadriceps strengthening exercise in patients with medial knee osteoarthritis and varus malalignment: a randomized controlled trial, *Arthritis Rheumatol.* 66 (4) (2014) 950–959, <https://doi.org/10.1002/art.38317>.
- [12] J. Schlicht, D.N. Camaione, S.V. Owen, Effect of intense strength training on standing balance, walking speed, and sit-to-stand performance in older adults, *J. Gerontol. A: Biol. Sci. Med. Sci.* 56 (5) (2001) M281–M286, <https://doi.org/10.1093/gerona/56.5.M281>.
- [13] E. van der Kruk, A.K. Silverman, P. Reilly, A.M.J. Bull, Compensation due to age-related decline in sit-to-stand and sit-to-walk, *J. Biomech.* 122 (2021) 110411, <https://doi.org/10.1016/j.jbiomech.2021.110411>.
- [14] M.E. Roebroek, C.A.M. Doorenbosch, J. Harlaar, R. Jacobs, G.J. Lankhorst, Biomechanics and muscular activity during sit-to-stand transfer, *Clin. Biomech.* 9 (4) (1994) 235–244, [https://doi.org/10.1016/0268-0033\(94\)90004-3](https://doi.org/10.1016/0268-0033(94)90004-3).
- [15] A.B. Schultz, N.B. Alexander, J.A. Ashton-Miller, Biomechanical analyses of rising from a chair, *J. Biomech.* 25 (12) (1992) 1383–1391, [https://doi.org/10.1016/0021-9290\(92\)90052-3](https://doi.org/10.1016/0021-9290(92)90052-3).
- [16] K. Mukund, S. Subramaniam, Skeletal muscle: a review of molecular structure and function, in health and disease, *Wiley Interdiscip. Rev.: Syst. Biol. Med.* 12 (1) (2020), <https://doi.org/10.1002/wsbm.1462>.
- [17] J. Allen, M. Ramsden, S. Nisar, Skeletal muscle structure, function and pathology, *Orthop. Trauma* 38 (3) (2024) 137–144, <https://doi.org/10.1016/j.mporth.2024.03.004>.
- [18] U. Trinler, K. Hollands, R. Jones, R. Baker, A systematic review of approaches to modelling lower limb muscle forces during gait: applicability to clinical gait analyses, *Gait. Posture* 61 (2018) 353–361, <https://doi.org/10.1016/j.gaitpost.2018.02.005>.
- [19] A. Erdemir, S. McLean, W. Herzog, A.J. van den Bogert, Model-based estimation of muscle forces exerted during movements, *Clin. Biomech. (Bristol Avon)* 22 (2) (2007) 131–154, <https://doi.org/10.1016/j.clinbiomech.2006.09.005>.
- [20] M.F. Miller, E. van der Kruk, A.K. Silverman, Age and initial position affect movement biomechanics in sit to walk transitions: lower limb muscle activity and joint moments, *J. Biomech.* 175 (October) (2024) 112367, <https://doi.org/10.1016/j.jbiomech.2024.112367>.
- [21] S. Yoshioka, A. Nagano, D.C. Hay, S. Fukashiro, The minimum required muscle force for a sit-to-stand task, *J. Biomech.* 45 (4) (2012) 699–705, <https://doi.org/10.1016/j.jbiomech.2011.11.054>.
- [22] E.J. Caruthers, J.A. Thompson, A.M.W. Chaudhari, et al., Muscle forces and their contributions to vertical and horizontal acceleration of the center of mass during sit-to-stand transfer in young, healthy adults, *J. Appl. Biomech.* 32 (5) (2016) 487–503, <https://doi.org/10.1123/jab.2015-0291>.
- [23] S.H.L. Smith, P. Reilly, A.M.J. Bull, A musculoskeletal modelling approach to explain sit-to-stand difficulties in older people due to changes in muscle recruitment and movement strategies, *J. Biomech.* 98 (2020) 109451, <https://doi.org/10.1016/j.jbiomech.2019.109451>.
- [24] J.J. Kutch, F.J. Valero-Cuevas, Muscle redundancy does not imply robustness to muscle dysfunction, *J. Biomech.* 44 (7) (2011) 1264–1270, <https://doi.org/10.1016/j.jbiomech.2011.02.014>.
- [25] B. Colom, J. Oliver, Garcia-Palmer FJ, Sexual dimorphism in the alterations of cardiac muscle mitochondrial bioenergetics associated to the ageing process, *J. Gerontol. - Biol. Sci. Med. Sci.* 70 (11) (2015) 1360–1369, <https://doi.org/10.1093/gerona/glu014>.
- [26] D.M. Callahan, T.W. Tourville, M.S. Miller, et al., Chronic disuse and skeletal muscle structure in older adults: sex-specific differences and relationships to contractile function, *Am. J. Physiol. - Cell Physiol.* 308 (11) (2015) C932–C943, <https://doi.org/10.1152/ajpcell.00014.2015>.
- [27] D.M. Callahan, N.G. Bedrin, M. Subramanian, et al., Age-related structural alterations in human skeletal muscle fibers and mitochondria are sex specific: relationship to single-fiber function, *J. Appl. Physiol.* 116 (12) (2014) 1582–1592, <https://doi.org/10.1152/jappphysiol.01362.2013>.
- [28] M. Brown, Sex and hormonal influences on skeletal muscle; differentiation and contractile mechanisms, *Adv. Mol. Cell Biol.* 34 (2004) 195–208, [https://doi.org/10.1016/S1569-2558\(03\)34014-7](https://doi.org/10.1016/S1569-2558(03)34014-7).
- [29] M.E. Rosa-Caldwell, N.P. Greene, Muscle metabolism and atrophy: let’s talk about sex, *Biol. Sex Differ.* 10 (1) (2019), <https://doi.org/10.1186/s13293-019-0257-3>.
- [30] M. Abdullah, A.A. Hulleck, R. Katmah, K. Khalaf, M. El-Rich, Multibody dynamics-based musculoskeletal modeling for gait analysis: a systematic review, *J. Neuroeng. Rehabil.* 21 (1) (2024) 178, <https://doi.org/10.1186/s12984-024-01458-y>.
- [31] S.K. Hunter, S.S. Angadi, A. Bhargava, et al., The biological basis of sex differences in athletic performance: consensus statement for the American College of Sports Medicine, *Transl. J. Am. Coll. Sports Med.* 8 (4) (2023) 1–33, <https://doi.org/10.1249/TJX.000000000000236>.
- [32] L.J. Anderson, H. Liu, J.M. Garcia, Sex differences in muscle wasting, in: *Advances in Experimental Medicine and Biology*, 1043, Springer, New York LLC, 2017, pp. 153–197, https://doi.org/10.1007/978-3-319-70178-3_9.
- [33] I. Janssen, S.B. Heymsfield, Z.M. Wang, R. Ross, Skeletal muscle mass and distribution in 468 men and women aged 18–88 yr, *J. Appl. Physiol.* 89 (1) (2000) 81–88, <https://doi.org/10.1152/jappphysiol.2000.89.1.81>.
- [34] A.E.J. Miller, J.D. MacDougall, M.A. Tarnopolsky, D.G. Sale, Gender differences in strength and muscle fiber characteristics, *Eur. J. Appl. Physiol. Occup. Physiol.* 66 (3) (1993) 254–262, <https://doi.org/10.1007/BF00235103>.
- [35] J.L. Nuzzo, Narrative review of sex differences in muscle strength, endurance, activation, size, Fiber type, and strength training participation rates, preferences, motivations, injuries, and neuromuscular adaptations, *J. Strength Cond. Res.* 37 (2) (2023) 494–536, <https://doi.org/10.1519/JSC.0000000000004329>.
- [36] C. Pizzolato, D.G. Lloyd, M. Sartori, et al., CEINMS: a toolbox to investigate the influence of different neural control solutions on the prediction of muscle excitation and joint moments during dynamic motor tasks, *J. Biomech.* 48 (14) (2015) 3929–3936, <https://doi.org/10.1016/j.jbiomech.2015.09.021>.
- [37] A. Ghazwan, C. Wilson, C.A. Holt, G.M. Whatling, Knee osteoarthritis alters periarthral knee muscle strategies during gait, *PLoS ONE* 17 (1 January) (2022), <https://doi.org/10.1371/journal.pone.0262798>.
- [38] S. Cabral, R. Fernandes, W.S. Selbie, V. Moniz-Pereira, A.P. Veloso, Inter-session agreement and reliability of the Global Gait Asymmetry index in healthy adults, *Gait. Posture* 51 (2017) 20–24, <https://doi.org/10.1016/j.gaitpost.2016.09.014>.
- [39] H.J. Hermens, B. Freriks, C. Disselhorst-Klug, G. Rau, Development of recommendations for SEMG sensors and sensor placement procedures, *J. Electromyogr. Kinesiol.* 10 (5) (2000) 361–374, [https://doi.org/10.1016/S1050-6411\(00\)00027-4](https://doi.org/10.1016/S1050-6411(00)00027-4).
- [40] C. Larivière, A. Delisle, A. Plamondon, The effect of sampling frequency on EMG measures of occupational mechanical exposure, *J. Electromyogr. Kinesiol.* 15 (2) (2005) 200–209, <https://doi.org/10.1016/J.JELEKIN.2004.08.009>.
- [41] J.C. Ives, J.K. Wigglesworth, Sampling rate effects on surface EMG timing and amplitude measures, *Clin. Biomech.* 18 (6) (2003) 543–552, [https://doi.org/10.1016/S0268-0033\(03\)00089-5](https://doi.org/10.1016/S0268-0033(03)00089-5).
- [42] A. Mantoan, C. Pizzolato, M. Sartori, Z. Sawacha, C. Cobelli, Reggiani M. MOTO-NMS, A MATLAB toolbox to process motion data for neuromusculoskeletal modeling and simulation, *Source Code Biol. Med.* 10 (1) (2015) 12, <https://doi.org/10.1186/s13029-015-0044-4>.
- [43] D.G. Lloyd, T.F. Besier, An EMG-driven musculoskeletal model to estimate muscle forces and knee joint moments in vivo, *J. Biomech.* 36 (6) (2003) 765–776, [https://doi.org/10.1016/S0021-9290\(03\)00010-1](https://doi.org/10.1016/S0021-9290(03)00010-1).
- [44] Perera C.K., Hussain Z., Khant M., Gopalai A.A., Gouwanda D., Human sitting to walking transitions: a motion capture dataset. [doi:10.26180/24515092.v3](https://doi.org/10.26180/24515092.v3).
- [45] A. Rajagopal, C.L. Dembia, M.S. DeMers, D.D. Delp, J.L. Hicks, S.L. Delp, Full-body musculoskeletal model for muscle-driven simulation of Human gait, *IEEE Trans. Biomed. Eng.* 63 (10) (2016) 2068–2079, <https://doi.org/10.1109/TBME.2016.2586891>.
- [46] S.L. Delp, F.C. Anderson, A.S. Arnold, et al., OpenSim: open-source software to create and analyze dynamic simulations of movement, *IEEE Trans. Biomed. Eng.* 54 (11) (2007) 1940–1950, <https://doi.org/10.1109/TBME.2007.901024>.
- [47] F.E. Zajac, Muscle and tendon: properties, models, scaling, and application to biomechanics and motor control, *Crit. Rev. Biomed. Eng.* 17 (4) (1989) 359–411.
- [48] D.C. Ackland, Y.C. Lin, M.G. Pandey, Sensitivity of model predictions of muscle function to changes in moment arms and muscle–tendon properties: a Monte-Carlo analysis, *J. Biomech.* 45 (8) (2012) 1463–1471, <https://doi.org/10.1016/j.jbiomech.2012.02.023>.
- [49] L. Modenese, E. Ceseracciu, M. Reggiani, D.G. Lloyd, Estimation of musculotendon parameters for scaled and subject specific musculoskeletal models using an optimization technique, *J. Biomech.* 49 (2) (2016) 141–148, <https://doi.org/10.1016/j.jbiomech.2015.11.006>.
- [50] M. Sartori, M. Reggiani, D. Farina, D.G. Lloyd, EMG-driven forward-dynamic estimation of muscle force and joint moment about multiple degrees of freedom in the Human lower extremity, *PLoS ONE* 7 (12) (2012), <https://doi.org/10.1371/journal.pone.0052618>.
- [51] D. Ao, M.M. Vega, M.S. Shourijeh, C. Patten, B.J. Fregly, EMG-driven musculoskeletal model calibration with estimation of unmeasured muscle excitations via synergy extrapolation, *Front. Bioeng. Biotechnol.* 10 (September) (2022) 1–23, <https://doi.org/10.3389/fbioe.2022.962959>.
- [52] N. Maniar, A.G. Schache, C. Pizzolato, D.A. Opar, Muscle function during single leg landing, *Sci. Rep.* 12 (1) (2022) 1–14, <https://doi.org/10.1038/s41598-022-15024-w>.
- [53] M. Sartori, D. Farina, D.G. Lloyd, Hybrid neuromusculoskeletal modeling to best track joint moments using a balance between muscle excitations derived from electromyograms and optimization, *J. Biomech.* 47 (15) (2014) 3613–3621, <https://doi.org/10.1016/j.jbiomech.2014.10.009>.
- [54] Perera C.K., Hussain Z., Khant M., Gopalai A.A., Gouwanda D., Ahmad S.A. A motion capture dataset on Human sitting to walking transitions. *Sci. Data.* [10.1038/s41597-024-03740-z](https://doi.org/10.1038/s41597-024-03740-z).
- [55] E. van der Kruk, P. Strutton, L.J. Koizia, M. Furtleman, P. Reilly, A.M.J. Bull, Why do older adults stand-up differently to young adults?: investigation of compensatory movement strategies in sit-to-walk, *npj Aging* 8 (1) (2022) 1–19, <https://doi.org/10.1038/s41514-022-00094-x>.
- [56] D.G. Lloyd, T.F. Besier, An EMG-driven musculoskeletal model to estimate muscle forces and knee joint moments in vivo, *J. Biomech.* 36 (6) (2003) 765–776, [https://doi.org/10.1016/S0021-9290\(03\)00010-1](https://doi.org/10.1016/S0021-9290(03)00010-1).
- [57] M. Sartori, M. Reggiani, D. Farina, D.G. Lloyd, EMG-driven forward-dynamic estimation of muscle force and joint moment about multiple degrees of freedom in the Human lower extremity, *PLOS ONE* 7 (12) (2012) e52618, <https://doi.org/10.1371/JOURNAL.PONE.0052618>.

- [58] G. Davico, D.G. Lloyd, C.P. Carty, B.A. Killen, D. Devaprakash, C. Pizzolato, Multi-level personalization of neuromusculoskeletal models to estimate physiologically plausible knee joint contact forces in children, *Biomech. Model. Mechanobiol.* 21 (6) (2022) 1873–1886, <https://doi.org/10.1007/s10237-022-01626-w>.
- [59] T.A. Buckley, C. Pitsikoulis, C.J. Hass, Dynamic postural stability during sit-to-walk transitions in Parkinson disease patients, *Mov. Disord.* 23 (9) (2008) 1274–1280, <https://doi.org/10.1002/mds.22079>.
- [60] A. Kerr, B. Durward, K.M. Kerr, Defining phases for the sit-to-walk movement, *Clin. Biomech.* 19 (4) (2004) 385–390, <https://doi.org/10.1016/j.clinbiomech.2003.12.012>.
- [61] L.N. Muhammad, Guidelines for repeated measures statistical analysis approaches with basic science research considerations, *J. Clin. Investig.* 133 (11) (2023), <https://doi.org/10.1172/JCI171058>.
- [62] G.D. Garson, Multilevel modeling: applications in STATA®, IBM® SPSS® SAS® R HLM™ (2023) <https://doi.org/10.4135/9781544319315>.
- [63] R.R. Neptune, S.A. Kautz, F.E. Zajac, Contributions of the individual ankle plantar flexors to support, forward progression and swing initiation during walking, *J. Biomech.* 34 (11) (2001) 1387–1398, [https://doi.org/10.1016/S0021-9290\(01\)00105-1](https://doi.org/10.1016/S0021-9290(01)00105-1).
- [64] M. Meinders, A. Gitter, J.M. Czerniecki, The role of ankle plantar flexor muscle work during walking, *Scand. J. Rehabil. Med.* 30 (1) (1998) 39–46, <https://doi.org/10.1080/003655098444309>.
- [65] K.L. Kendall, C.M. Fairman, Women and exercise in aging, *J. Sport Health Sci.* 3 (3) (2014) 170–178, <https://doi.org/10.1016/j.jshs.2014.02.001>.
- [66] Y. Chen, C. Jin, H. Tang, et al., Effects of sedentary behaviour and long-term regular Tai Chi exercise on dynamic stability control during gait initiation in older women, *Front. Bioeng. Biotechnol.* 12 (May) (2024) 1–10, <https://doi.org/10.3389/fbioe.2024.1353270>.
- [67] B. Moreland, R. Kakara, A. Henry, Trends in nonfatal falls and fall-related injuries among adults aged ≥ 65 years — United States, 2012–2018, *MMWR Morb. Mortal. Wkly. Rep.* 69 (27) (2020) 875–881, <https://doi.org/10.15585/mmwr.mm6927a5>.
- [68] E. van der Kruk, A.K. Silverman, L. Koizia, P. Reilly, M. Fertleman, A.M.J. Bull, Age-related compensation: neuromusculoskeletal capacity, reserve & movement objectives, *J. Biomech.* 122 (2021) 110385, <https://doi.org/10.1016/j.jbiomech.2021.110385>.
- [69] K. Keller, M. Engelhardt, Strength and muscle mass loss with aging process. Age and strength loss, *Muscles Ligaments Tendons J.* 3 (4) (2013) 346–350, <https://doi.org/10.11138/mltj/2013.3.4.346>.
- [70] E. Volpi, R. Nazemi, S. Fujita, Muscle tissue changes with aging, *Curr. Opin. Clin. Nutr. Metab. Care* 7 (4) (2004) 405–410, <https://doi.org/10.1097/01.mco.0000134362.76653.b2>.
- [71] S.D. Uhlich, R.W. Jackson, A. Seth, J.A. Kolesar, S.L. Delp, Muscle coordination retraining inspired by musculoskeletal simulations reduces knee contact force, *Sci. Rep.* 12 (1) (2022) 1–13, <https://doi.org/10.1038/s41598-022-13386-9>.
- [72] C.J. Hass, R.J. Gregor, D.E. Waddell, et al., The influence of Tai Chi training on the center of pressure trajectory during gait initiation in older adults, *Arch. Phys. Med. Rehabil.* 85 (10) (2004) 1593–1598, <https://doi.org/10.1016/j.apmr.2004.01.020>.
- [73] K.M. Steele, M.S. DeMers, M.S. Schwartz, S.L. Delp, Compressive tibiofemoral force during crouch gait: supplementary information, *Gait. Posture* 35 (4) (2012) 21–26.
- [74] K.J. Bennett, C. Pizzolato, S. Martelli, et al., EMG-informed neuromusculoskeletal models accurately predict knee loading measured using instrumented implants, *IEEE Trans. Biomed. Eng.* 69 (7) (2022) 2268–2275, <https://doi.org/10.1109/TBME.2022.3141067>.
- [75] P. Ortega-Bastidas, P. Aqueveque, B. Gómez, F. Saavedra, R. Cano-De-La-Cuerda, Use of a single wireless IMU for the segmentation and automatic analysis of activities performed in the 3-m timed up & go test, *Sens. (Switz.)* 19 (7) (2019) 1647, <https://doi.org/10.3390/s19071647>.